



Możliwości wytworzenia pierwiastków o $Z > 118$

Autor Autor

T. Cap



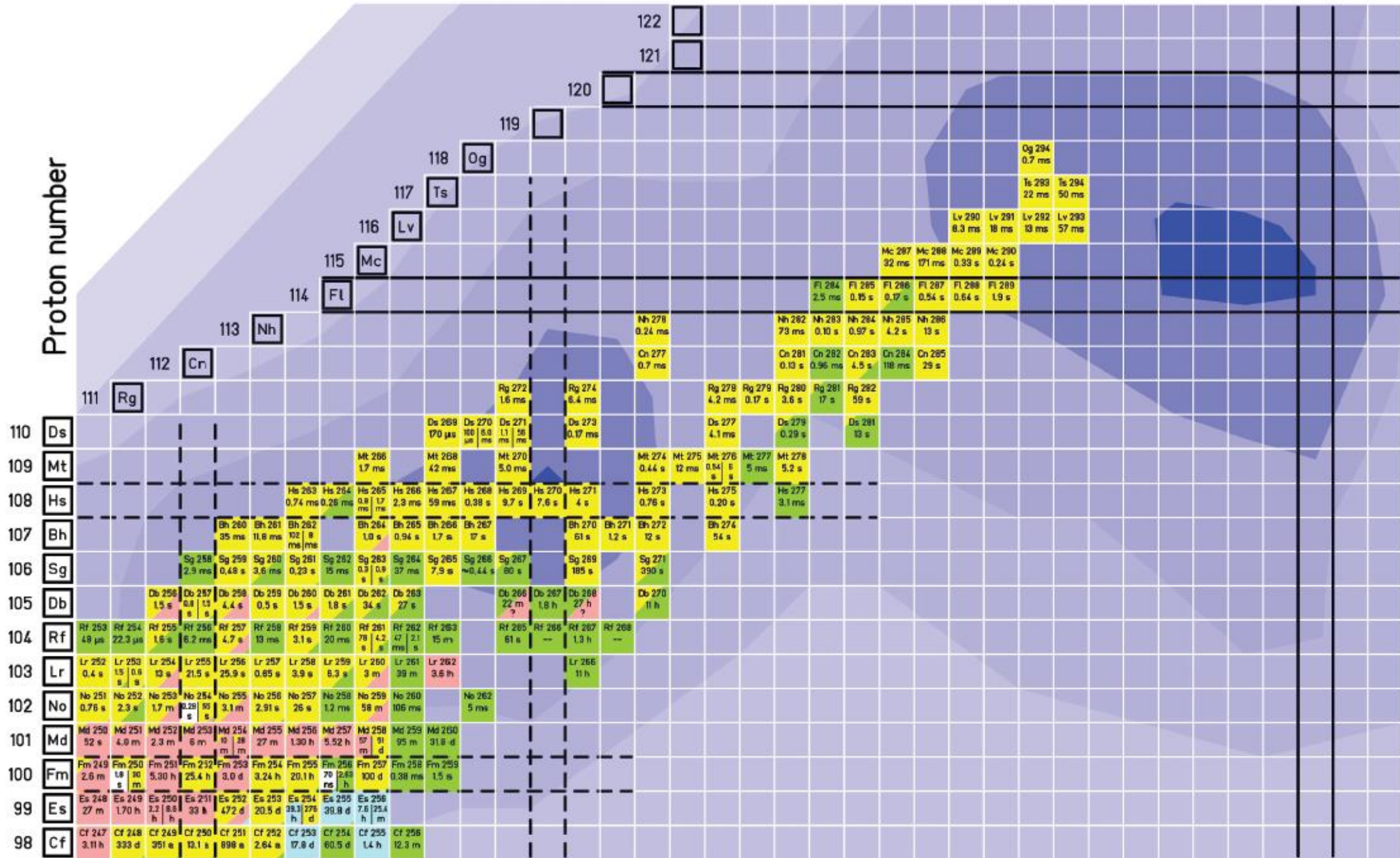
NATIONAL
CENTRE
FOR NUCLEAR
RESEARCH
ŚWIERK

Seminarium
Wydział Fizyki UW, 01.12.22

1																	18
H ₁											B ₅	C ₆	N ₇	O ₈	F ₉	He ₂	
Li ₃	Be ₄											Al ₁₃	Si ₁₄	P ₁₅	S ₁₆	Cl ₁₇	Ar ₁₈
Na ₁₁	Mg ₁₂	Sc ₂₁	Ti ₂₂	V ₂₃	Cr ₂₄	Mn ₂₅	Fe ₂₆	Co ₂₇	Ni ₂₈	Cu ₂₉	Zn ₃₀	Ga ₃₁	Ge ₃₂	As ₃₃	Se ₃₄	Br ₃₅	Kr ₃₆
Rb ₃₇	Sr ₃₈	Y ₃₉	Zr ₄₀	Nb ₄₁	Mo ₄₂	Tc ₄₃	Ru ₄₄	Rh ₄₅	Pd ₄₆	Ag ₄₇	Cd ₄₈	In ₄₉	Sn ₅₀	Sb ₅₁	Te ₅₂	I ₅₃	Xe ₅₄
Cs ₅₅	Ba ₅₆	La-Lu ₅₇₋₇₁	Hf ₇₂	Ta ₇₃	W ₇₄	Re ₇₅	Os ₇₆	Ir ₇₇	Pt ₇₈	Au ₇₉	Hg ₈₀	Tl ₈₁	Pb ₈₂	Bi ₈₃	Po ₈₄	At ₈₅	Rn ₈₆
Fr ₈₇	Ra ₈₈	Ac-Lr ₈₉₋₁₀₃	Rf ₁₀₄	Db ₁₀₅	Sg ₁₀₆	Bh ₁₀₇	Hs ₁₀₈	Mt ₁₀₉	Ds ₁₁₀	Rg ₁₁₁	Cn ₁₁₂	Nh ₁₁₃	Fl ₁₁₄	Mc ₁₁₅	Lv ₁₁₆	Ts ₁₁₇	Og ₁₁₈
(Uue) ₍₁₁₉₎	(Ubn) ₍₁₂₀₎																
Lanthanides	La ₅₇	Ce ₅₈	Pr ₅₉	Nd ₆₀	Pm ₆₁	Sm ₆₂	Eu ₆₃	Gd ₆₄	Tb ₆₅	Dy ₆₆	Ho ₆₇	Er ₆₈	Tm ₆₉	Yb ₇₀	Lu ₇₁		
Actinides	Ac ₈₉	Th ₉₀	Pa ₉₁	U ₉₂	Np ₉₃	Pu ₉₄	Am ₉₅	Cm ₉₆	Bk ₉₇	Cf ₉₈	Es ₉₉	Fm ₁₀₀	Md ₁₀₁	No ₁₀₂	Lr ₁₀₃		

Discovery of a chemical element is the experimental demonstration, beyond reasonable doubt, of the existence of a nuclide with an atomic number Z not identified before, existing for at least 10^{-14} s.

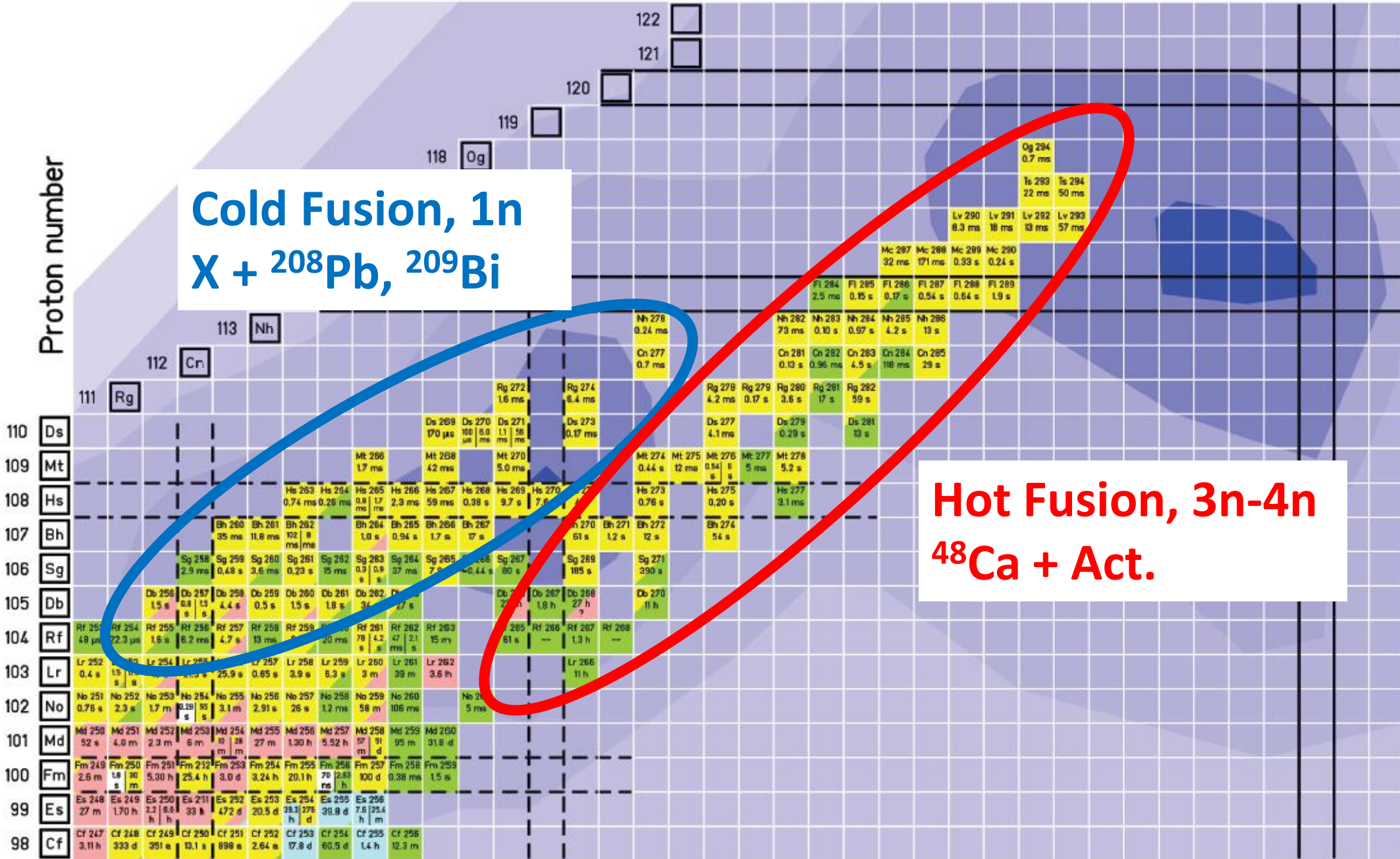
Proton number



Proton number

Cold Fusion, 1n
 $X + {}^{208}\text{Pb}, {}^{209}\text{Bi}$

Hot Fusion, 3n-4n
 ${}^{48}\text{Ca} + \text{Act.}$

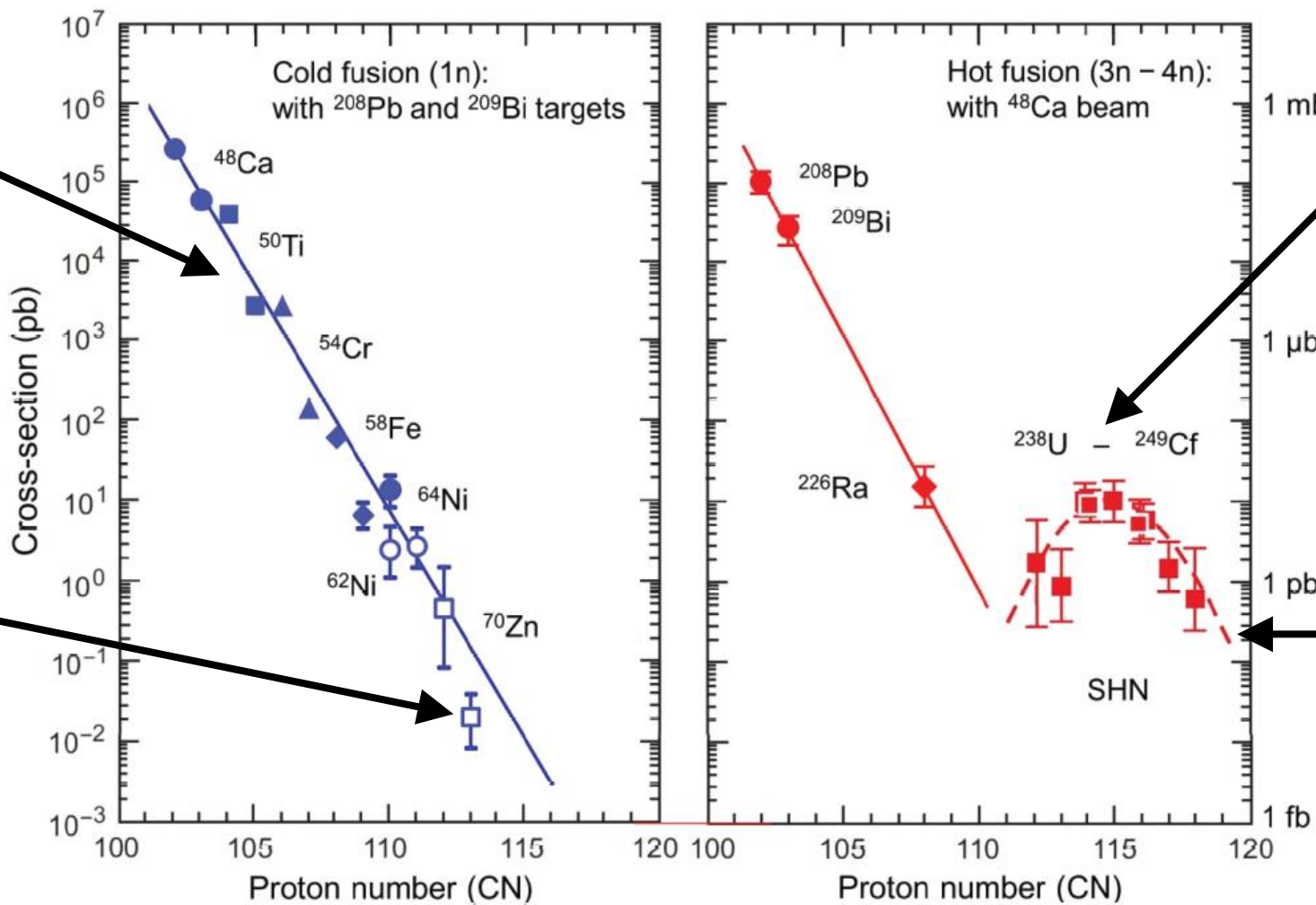


149 150 151 152 153 154 155 156 157 158 159 160 161 162 163 164 165 166 167 168 169 170 171 172 173 174 175 176 177 178 179 180 181 182 183 184 185 186

Neutron number

Cross section drops 7 orders of magnitude with the change from Ca to Zn.

Z=113, 22 fb, only 3 atoms in 576 days of irradiation



No heavier target than Cf (Z=98) is available.

Es (Z=99) is too radioactive but can possibly be used.

Experiments with ^{50}Ti , ^{54}Cr , ^{58}Fe and ^{64}Ni beams have not succeeded so far.

Sigurd Hofmann, Sergey N. Dmitriev, Claes Fahlander, Jacklyn M. Gates, James B. Roberto and Hideyuki Sakai
Report of the 2017 Joint Working Group of IUPAC and IUPAP, Pure Appl. Chem. 2020; 92(9): 1387–1446

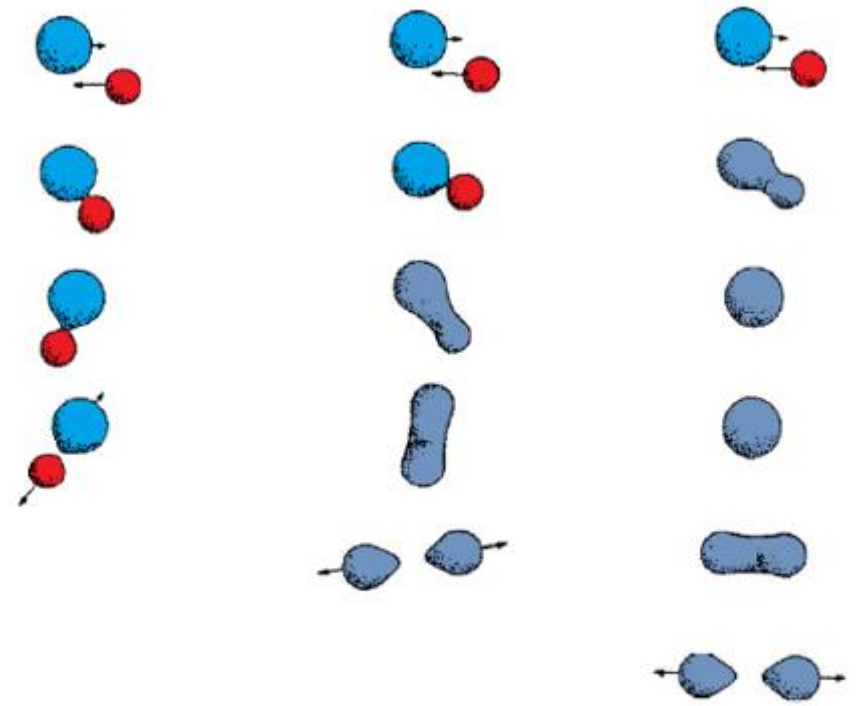
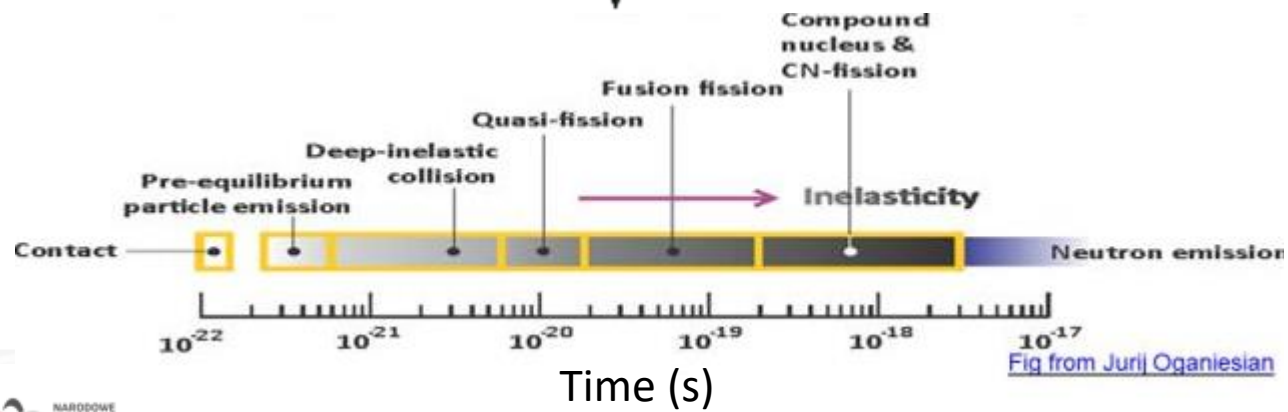
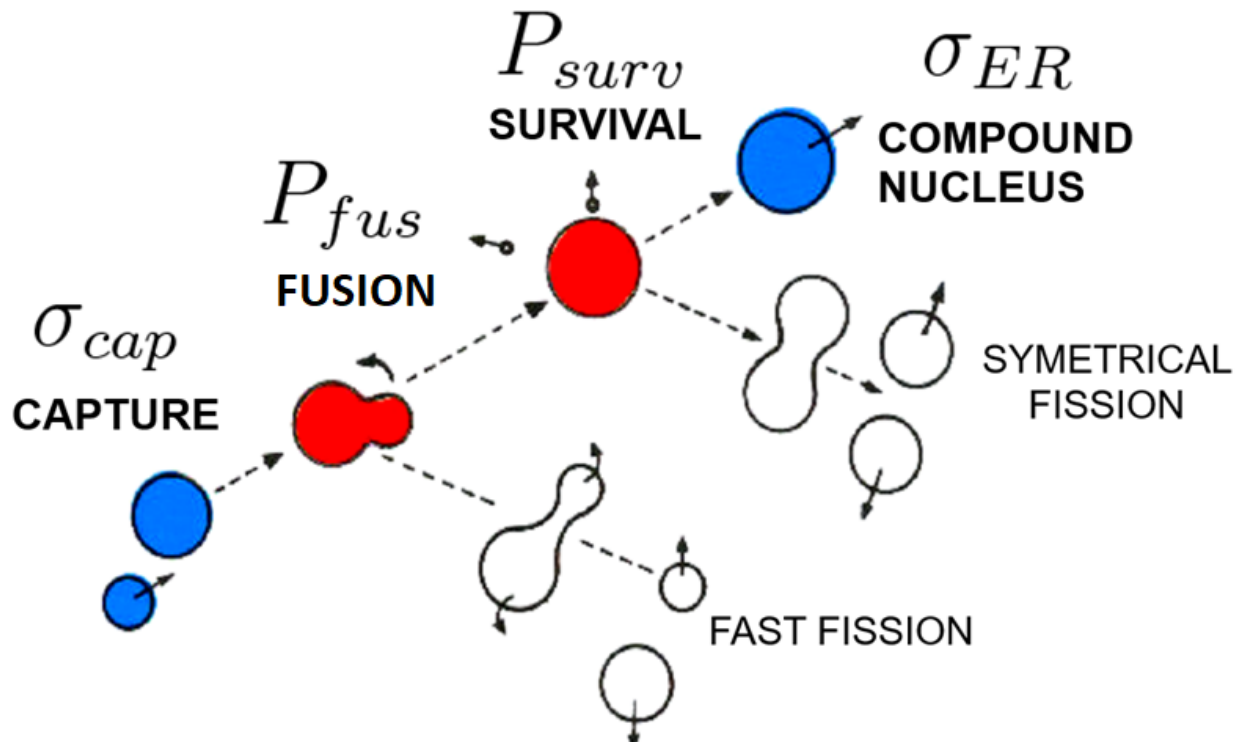
Hot fusion synthesis experiments leading to elements 119 and 120

$^{48}\text{Ca} + ^{254}\text{Es} \rightarrow ^{302}\mathbf{119}^*$ Limit of 300 nb R. W. Lougheed *et al.*, Phys. Rev. C **32**, 1760 (1985)

$^{50}\text{Ti} + ^{249}\text{Bk} \rightarrow ^{299}\mathbf{119}^*$ Limit of 65 fb J. Khuyagbaatar *et al.*, Phys. Rev. C **102**, 064602 (2020)
 $^{51}\text{V} + ^{248}\text{Cm} \rightarrow ^{299}\mathbf{119}^*$ ongoing experiment in RIKEN

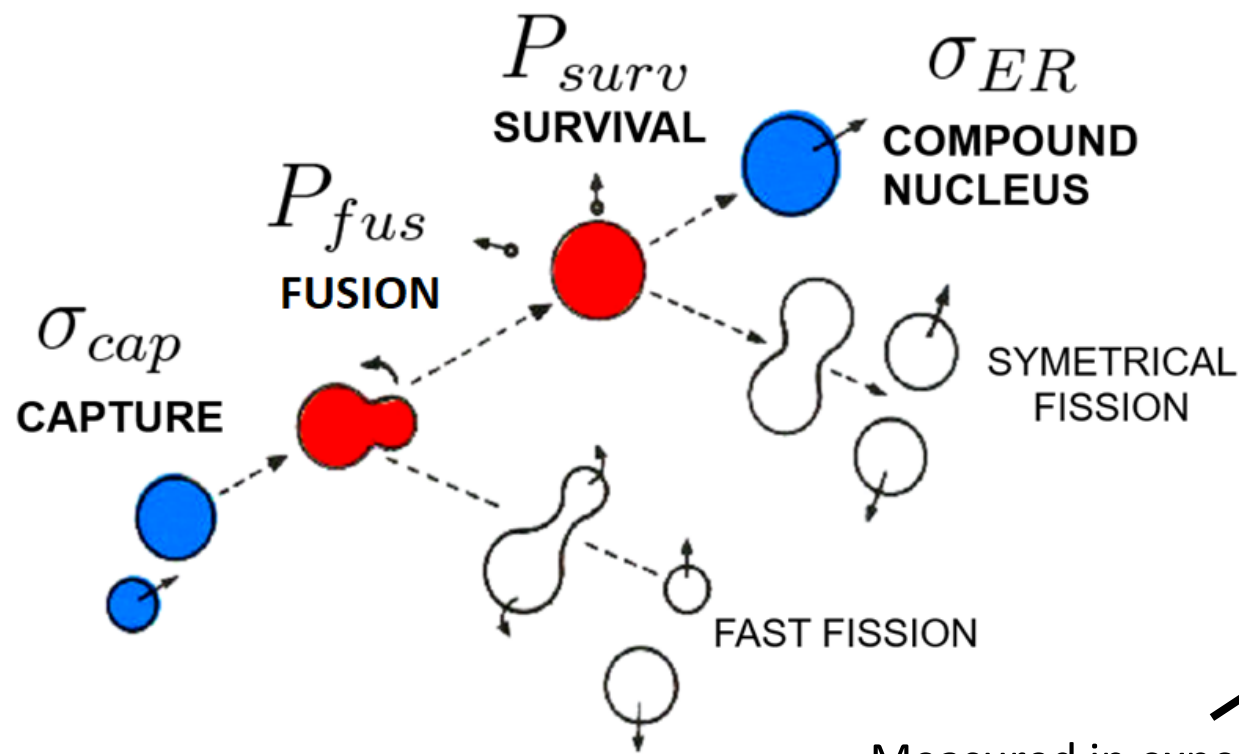
$^{50}\text{Ti} + ^{249}\text{Cf} \rightarrow ^{299}\mathbf{120}^*$ Limit of 200 fb J. Khuyagbaatar *et al.*, Phys. Rev. C **102**, 064602 (2020)
 $^{58}\text{Fe} + ^{244}\text{Pu} \rightarrow ^{302}\mathbf{120}^*$ Limit of 400 fb Yu. Ts. Oganessian *et al.*, Phys. Rev. C **79**, 024603 (2009)
 $^{64}\text{Ni} + ^{238}\text{U} \rightarrow ^{302}\mathbf{120}^*$ Limit of 90 fb S. Hoffmann *et al.*, GSI Report 2009-1
 $^{54}\text{Cr} + ^{248}\text{Cm} \rightarrow ^{302}\mathbf{120}^*$ Limit of 580 fb S. Hoffmann *et al.*, Eur. Phys. J. A **52**, 180 (2016)

Different mass – angle correlations and different TKE



DEEP INELASTIC SCATTERING QUASIFISSION FUSION-FISSION

$$\sigma_{ER} = \sigma_{cap} P_{fus} P_{surv}$$



FBD (fusion-by-diffusion)

Synthesis of SHN can be described as a **3** step process:

$$\sigma_{ER} = \sigma_{cap} \times P_{fus} \times P_{surv}$$

Not measured directly,
difficult to calculate

Measured in experiments, can be
calculated using various models

Well established theory and
formulas
Monte Carlo Statistical model

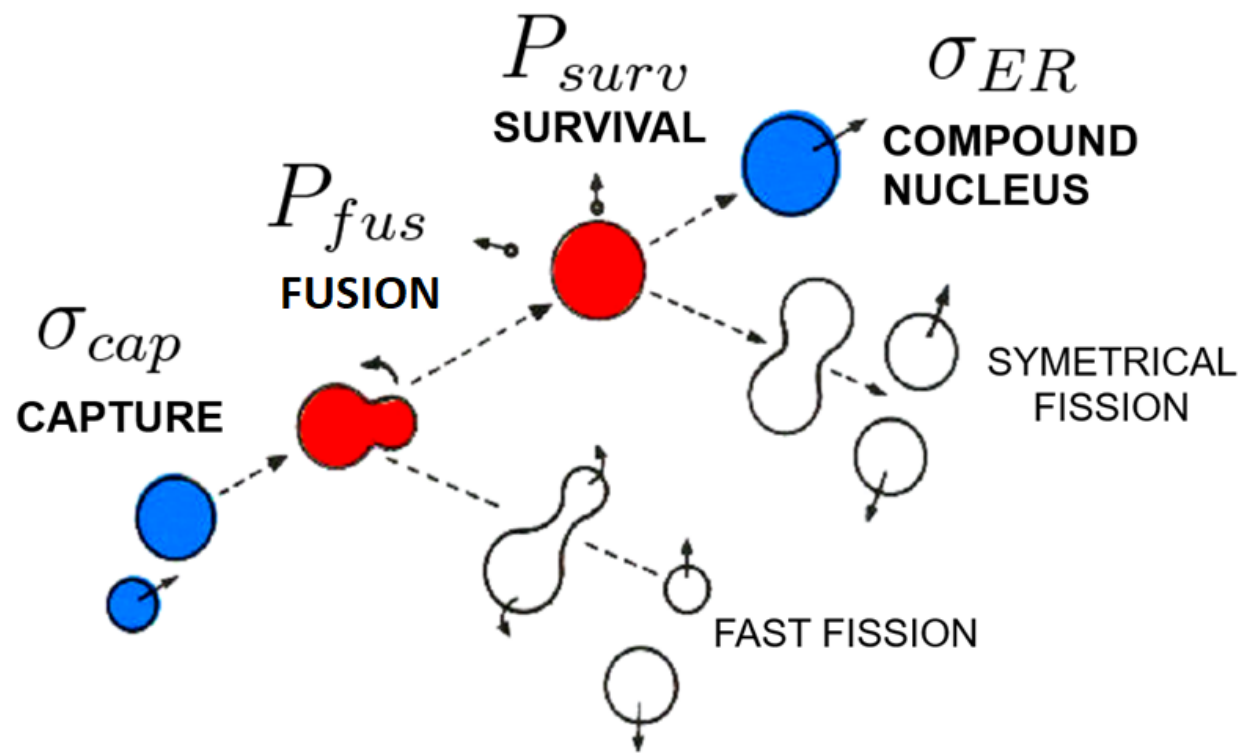
**Smoluchowski
Diffusion
Equation**

**masses, fission barriers,
deformations from Warsaw
Micro-Macro model**

**Diffused barrier formula
(Entrance channel barrier is given
by a Gaussian distribution)**

W. J. Świątecki, K. Siwek-Wilczyńska,
J. Wilczyński, **PRC 2005**

T. Cap et al., **PRC 2011**
K. Siwek-Wilczyńska et al. **PRC 2012**
T. Cap et al., **PRC 2013**
K. Siwek-Wilczyńska et al. **PRC 2019**



FBD (fusion-by-diffusion)

Synthesis of SHN can be described as a **3** step process:

$$\sigma_{ER} = \sigma_{cap} P_{fus} P_{surv}$$



l -dependent FBD

$$\sigma_{ER} = \pi \hat{\lambda}^2 \sum_{l=0}^{\infty} (2l + 1) T(l) \times P_{fus}(l) \times P_{surv}^{xn}(l)$$

W. J. Świątecki, K. Siwek-Wilczyńska,
J. Wilczyński, **PRC 2005**

T. Cap et al., **PRC 2011**

K. Siwek-Wilczyńska et al. **PRC 2012**

T. Cap et al., **PRC 2013**

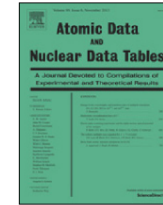
K. Siwek-Wilczyńska et al. **PRC 2019**



Contents lists available at [ScienceDirect](https://www.sciencedirect.com)

Atomic Data and Nuclear Data Tables

journal homepage: www.elsevier.com/locate/adt



Properties of heaviest nuclei with $98 \leq Z \leq 126$ and $134 \leq N \leq 192$

P. Jachimowicz^a, M. Kowal^{b,*}, J. Skalski^b

^a Institute of Physics, University of Zielona Góra, Szafrana 4a, 65-516 Zielona Góra, Poland

^b National Centre for Nuclear Research, Pasteura 7, 02-093 Warsaw, Poland



Ground-state and saddle-point shapes and masses for 1305 heavy and superheavy nuclei

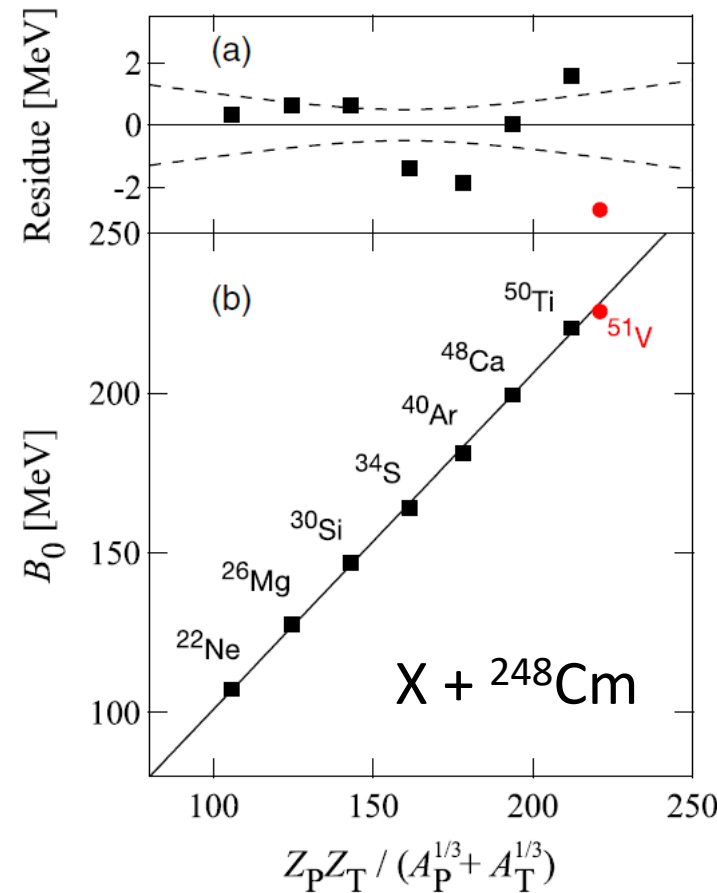
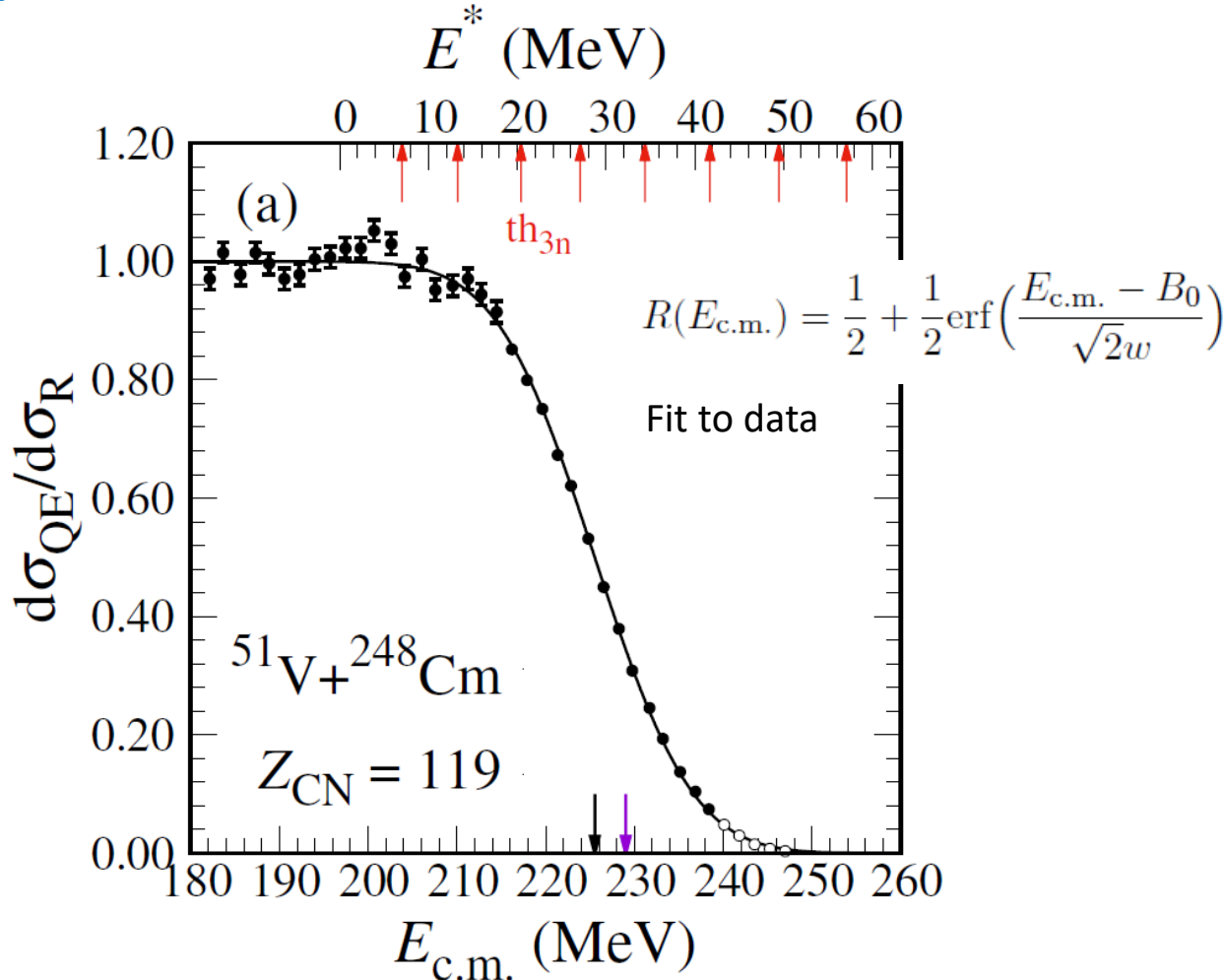
including odd-A and odd–odd systems. Static fission barrier heights, one- and two-nucleon separation energies, and $Q\alpha$ values.

Microscopic–macroscopic method with the deformed Woods–Saxon single-particle potential and the Yukawa-plus-exponential macroscopic energy taken as the smooth part.

Ground-state shapes and energies are found by the minimization over **seven axially-symmetric deformations**. A search for saddle-points was performed by using the "imaginary water flow" method in three consecutive stages, using five- (for nonaxial shapes) and seven-dimensional (for reflection-asymmetric shapes) deformation spaces.

Good agreement with the experimental data for actinides.

capture cross section for $^{51}\text{V} + ^{248}\text{Cm}$



B_0 from the FBD is in agreement with the systematics, which gives:

$$228.3 \pm 1.1 \text{ MeV}$$

and 3.5 MeV above the exp. value

M. Tanaka *et al.*: $B_0 = 225.6 \pm 0.2 \text{ MeV}$

Fit to data: $B_0 = 225.53 \pm 0.13 \text{ MeV}$ $\omega = 8.71 \pm 0.18 \text{ MeV}$

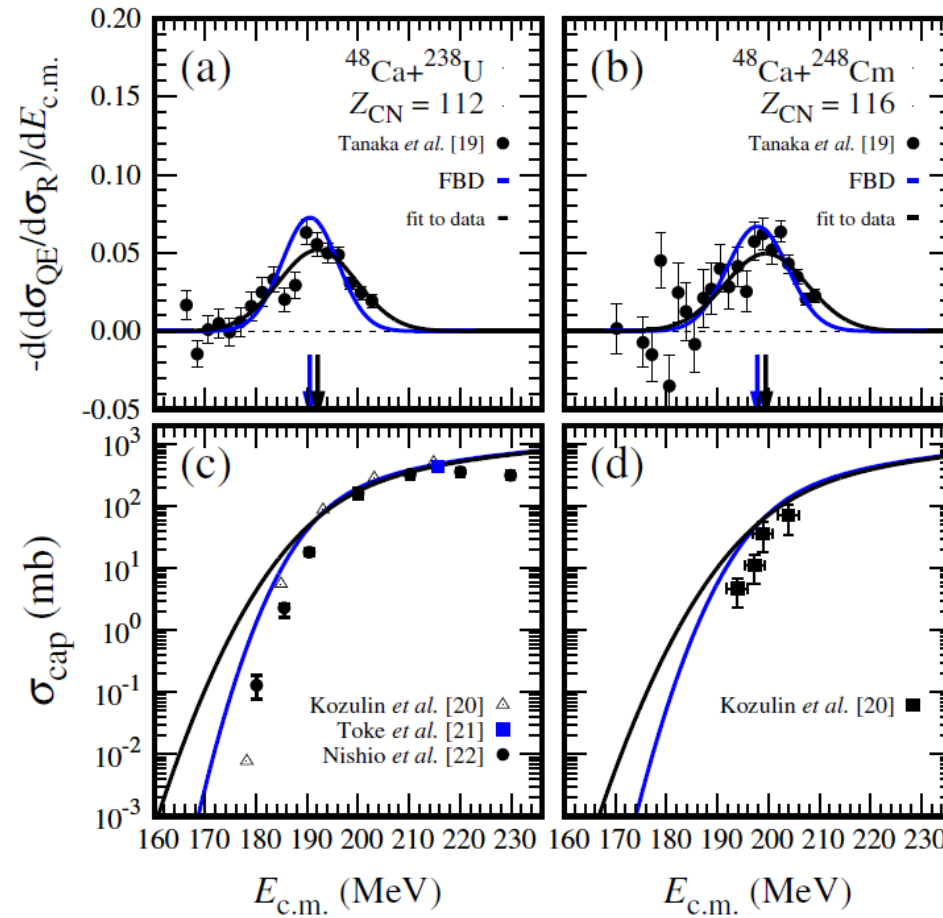
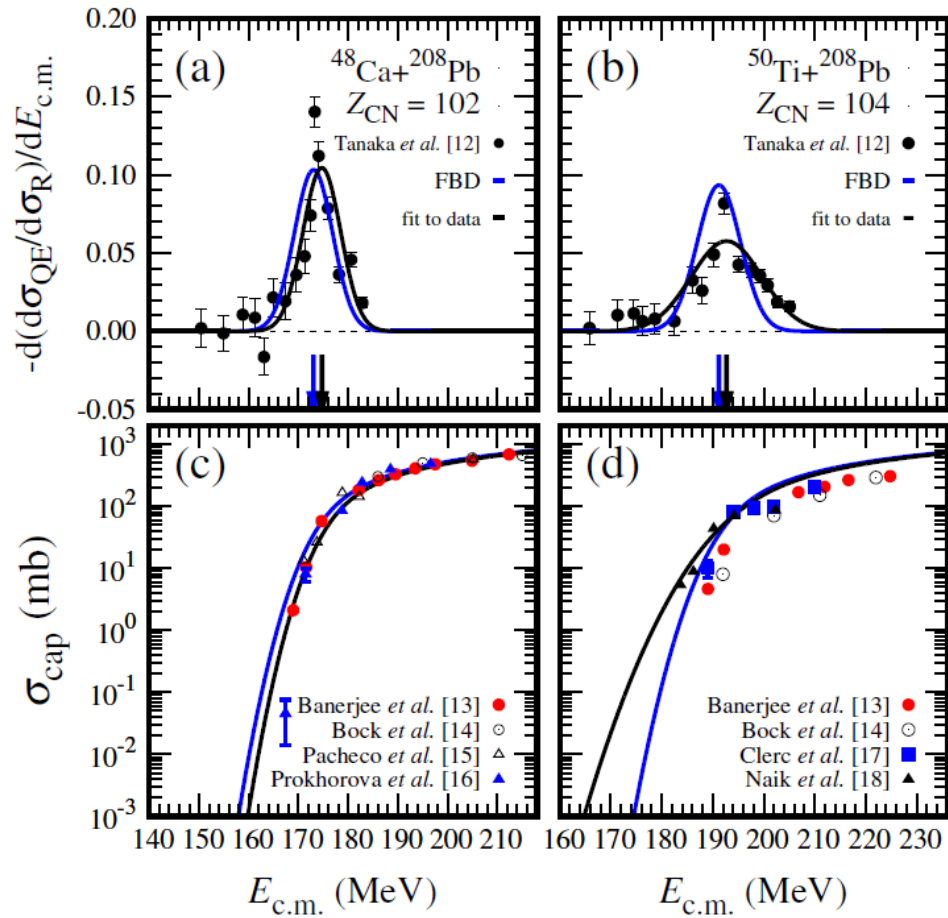
FBD model: $B_0 = 229.03 \text{ MeV}$ $\omega = 6.90 \text{ MeV}$ (only β_2 Cm deformation)

Data taken from:

M. Tanaka *et al.*, J. Phy. Soc. Jpn 91, 084201 (2022)

capture cross section

$$D(B) = \frac{1}{\sqrt{2\pi}\omega} \exp\left(-\frac{(B-B_0)^2}{2\omega^2}\right)$$



Barrier dist. data taken from:

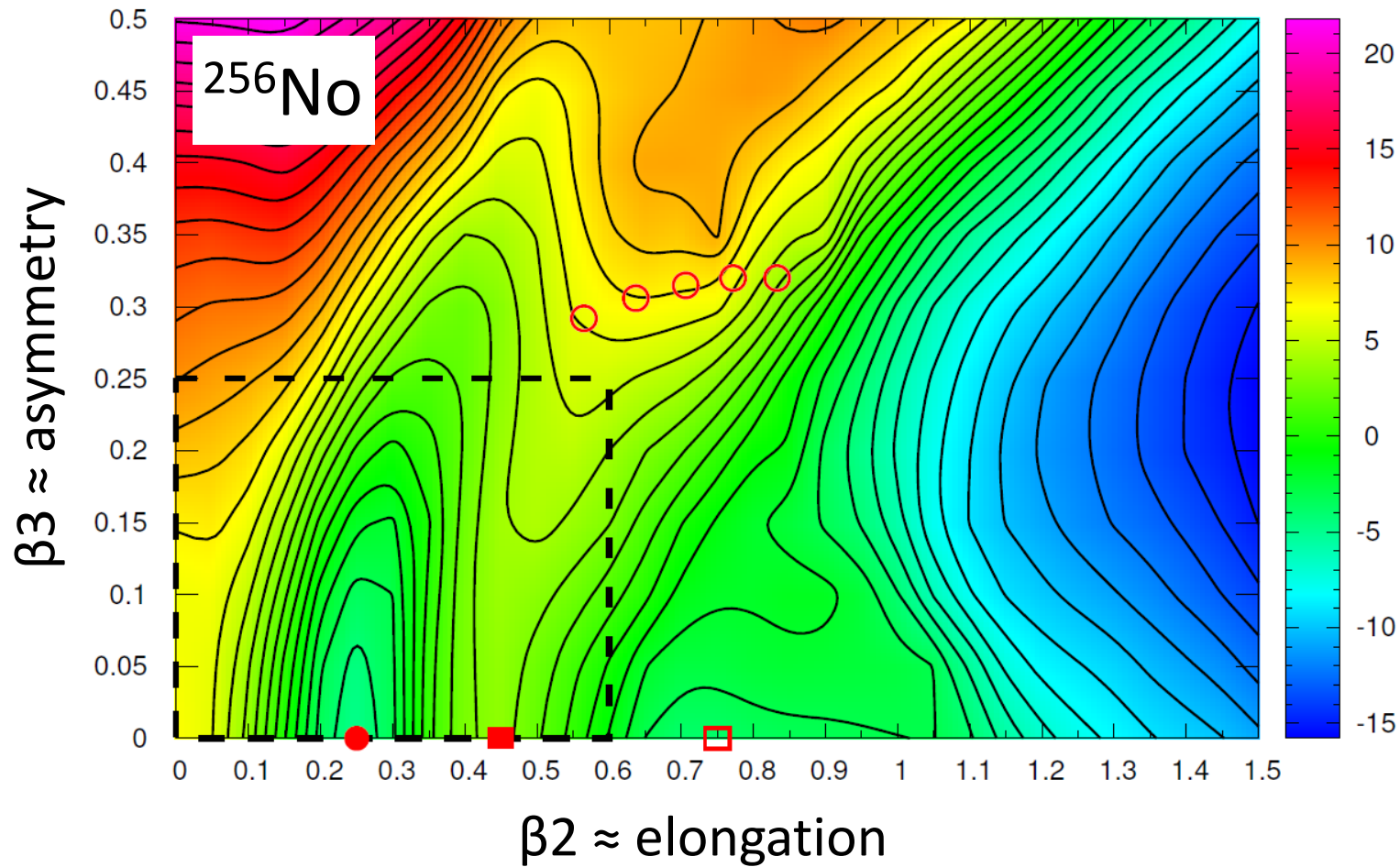
T. Tanaka *et al.*, J. Phy. Soc. Jpn 87, 014201, 2018

T. Tanaka *et al.*, PRL 124, 052502, 2020

$$\sigma_{cap}(E_{c.m.}) = \pi R^2 \frac{w}{\sqrt{2\pi} E_{c.m.}} \left[\sqrt{\pi} X (1 + \text{erf} X) + \exp(-X^2) \right]$$

Fusion process on the Potential Energy Surface (PES)

$$E(\beta) = \text{Binding Energy} - E(\text{sphere})$$



Macro-Micro model

P. Jachimowicz, M. Kowal

and J. Skalski

ADNDT 138, 101393 (2021)

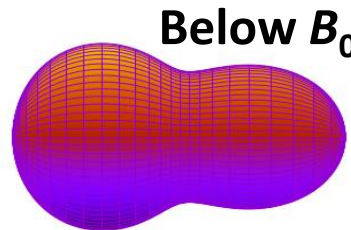
$\beta_1 - \beta_8$ deformation space

β_1 – real shape variable

2D representation of 8D
deformation space (124M point)

Calculations done by
Aleksander Augustyn in CIŚ
(Świerk Computing Centre)

Fusion starting point
(injection point)
 $^{48}\text{Ca} + ^{208}\text{Pb} \rightarrow ^{256}\text{No}$



Macro-Micro model

P. Jachimowicz, M. Kowal
and J. Skalski

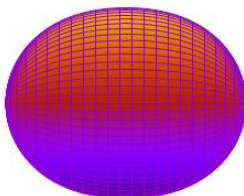
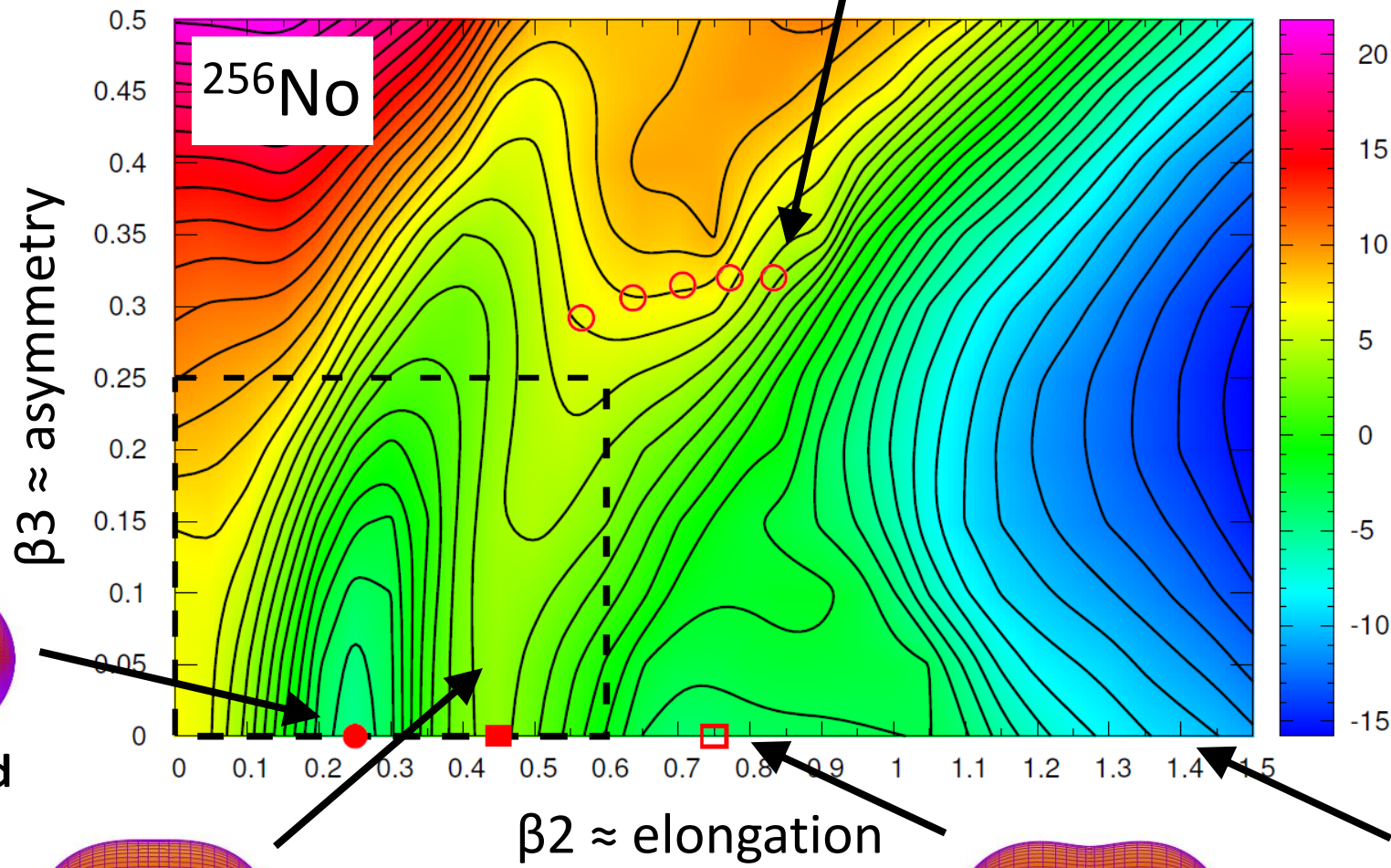
ADNDT 138, 101393 (2021)

$\beta_1 - \beta_8$ deformation space

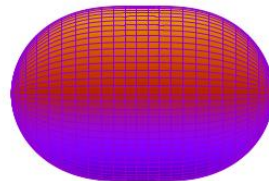
β_1 - real shape variable

2D representation of 8D
deformation space (124M point)

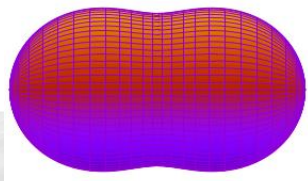
Calculations done by
Aleksander Augustyn in CIŚ
(Świerk Computing Centre)



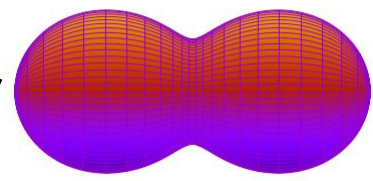
Compound
nucleus



Fission saddle point



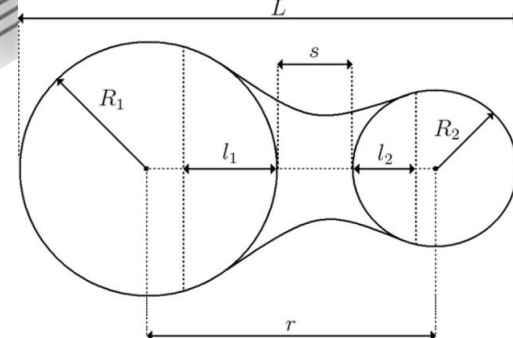
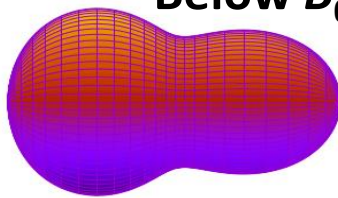
2nd minimum



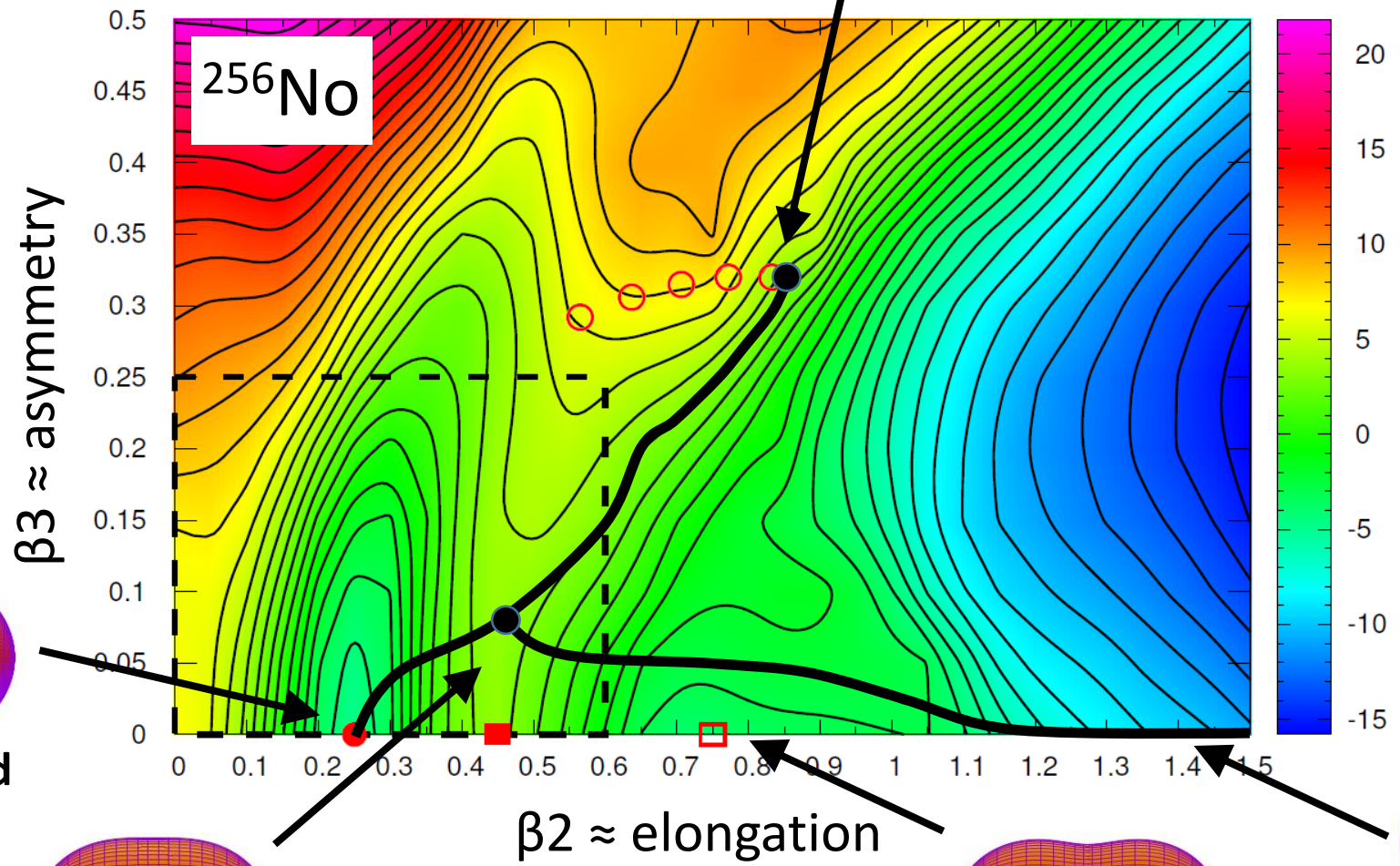
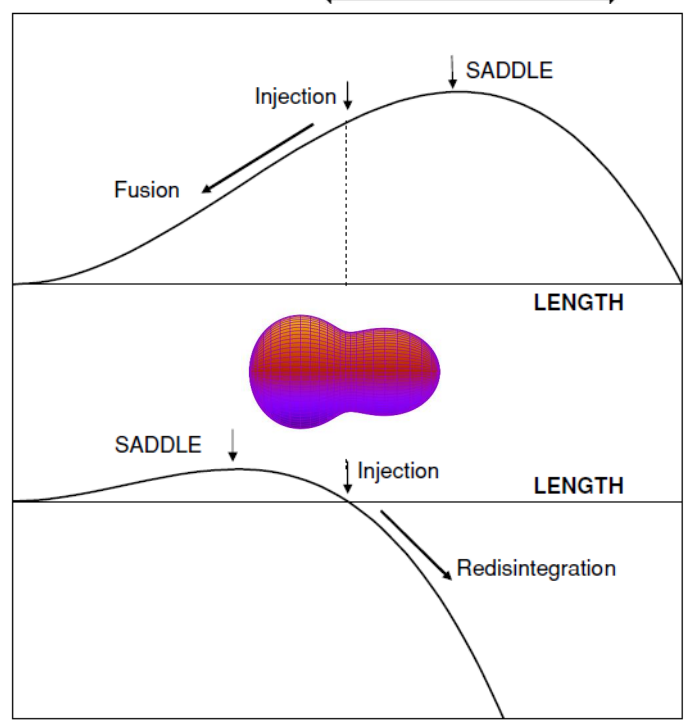
Scission point
symmetric fission

Fusion starting point
(injection point)
 $^{48}\text{Ca} + ^{208}\text{Pb} \rightarrow ^{256}\text{No}$

Below B_0



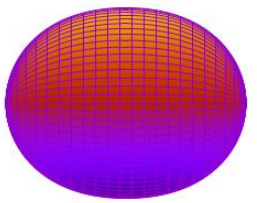
FBD



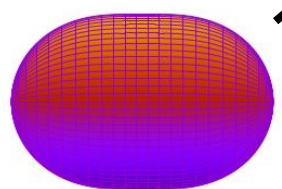
^{256}No

$\beta_3 \approx$ asymmetry

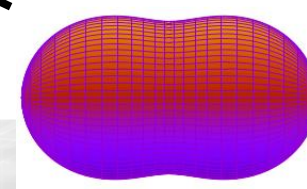
$\beta_2 \approx$ elongation



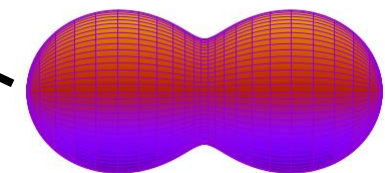
Compound nucleus



Fission saddle point



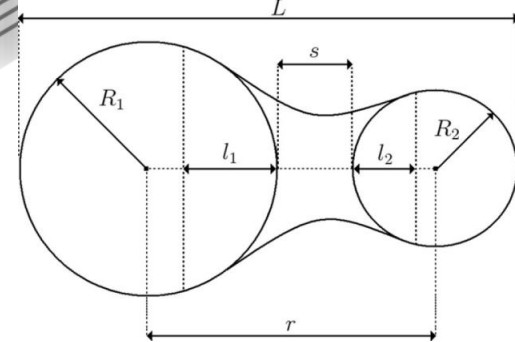
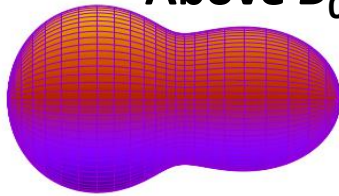
2nd minimum



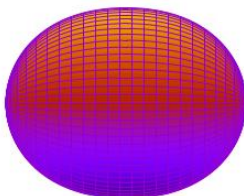
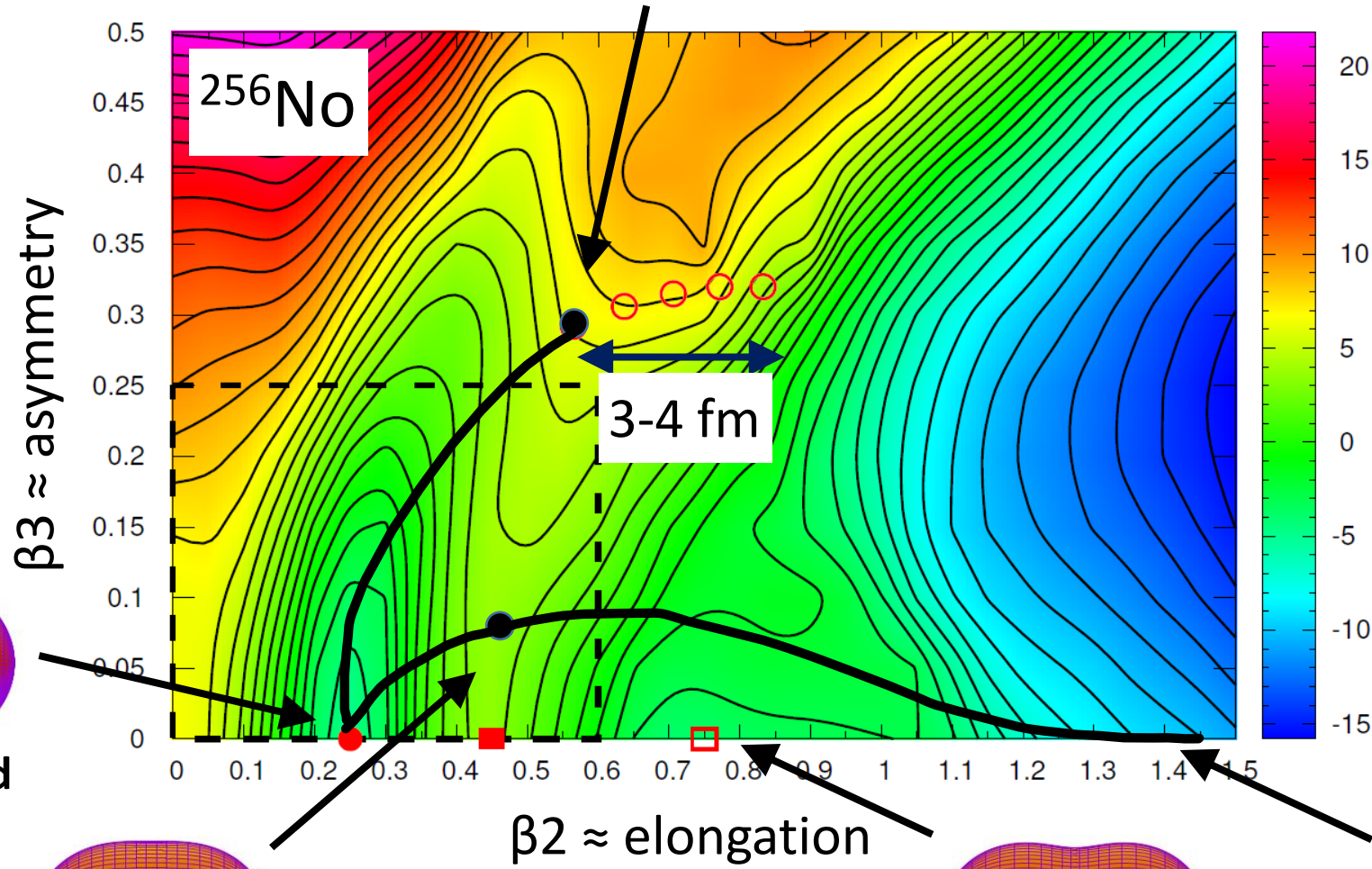
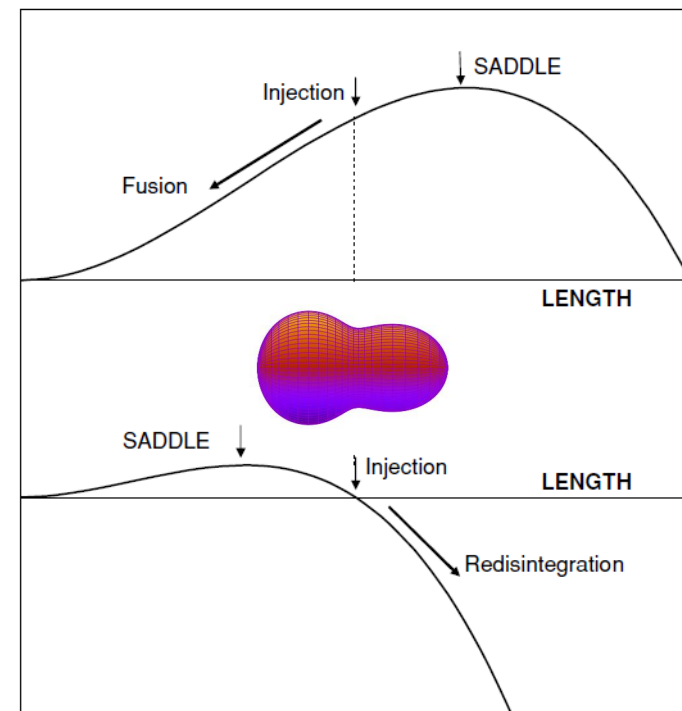
Scission point
symmetrical fission

Fusion starting point
(injection point)
 $^{48}\text{Ca} + ^{208}\text{Pb} \rightarrow ^{256}\text{No}$

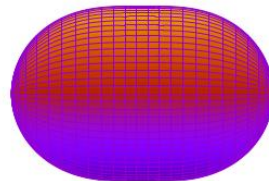
Above B_0



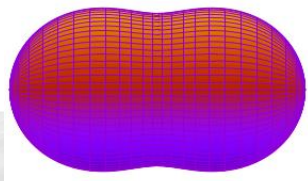
FBD



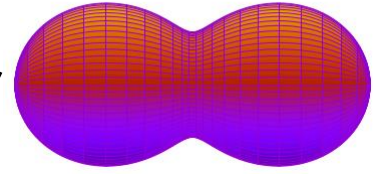
Compound nucleus



Fission saddle point

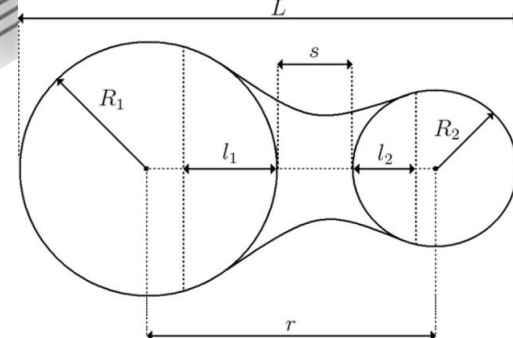
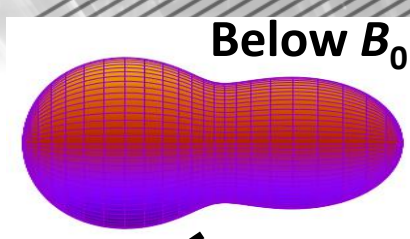
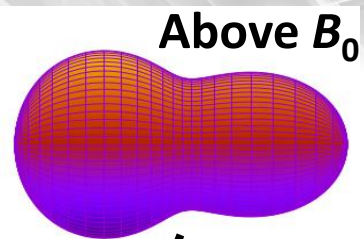


2nd minimum

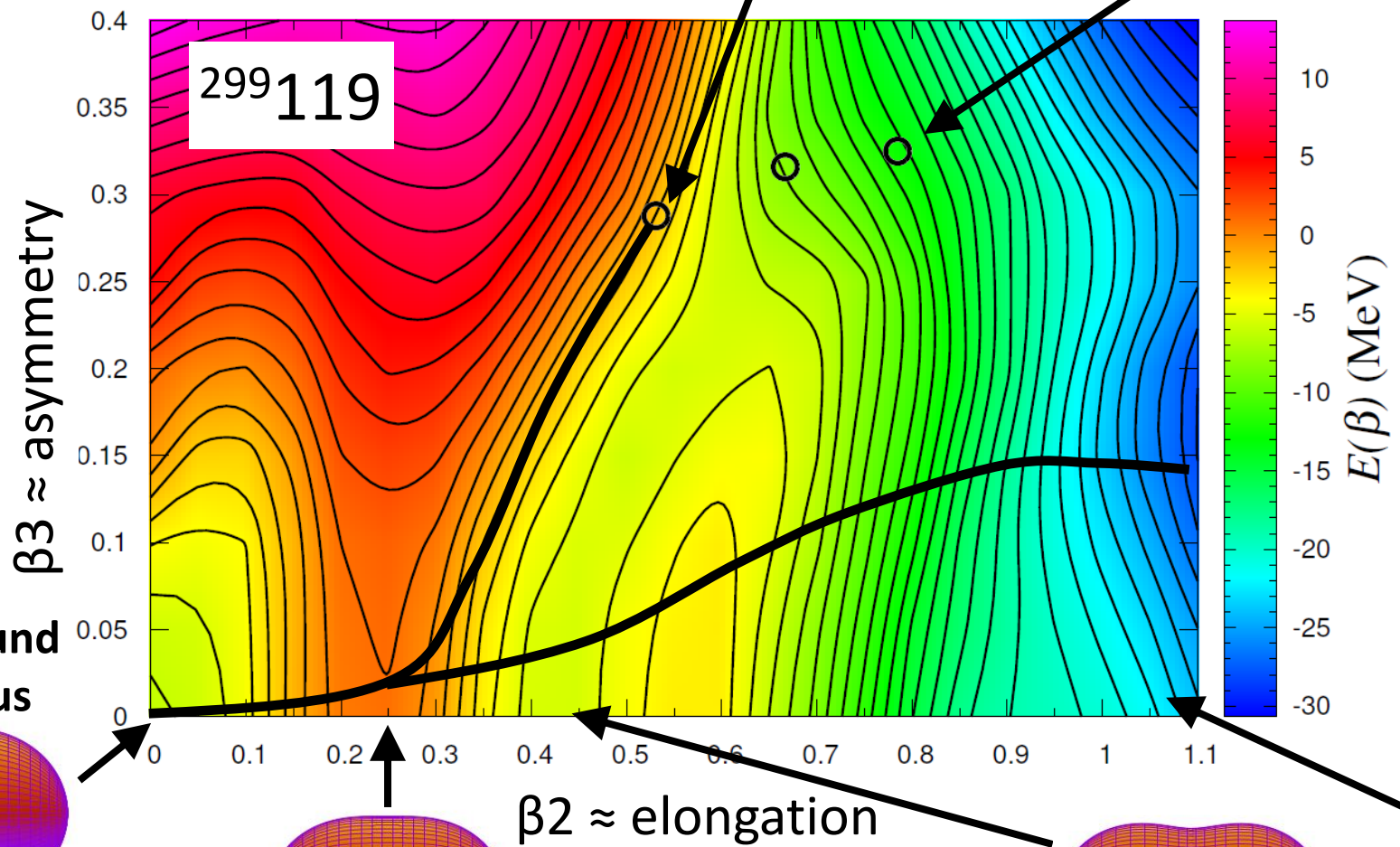
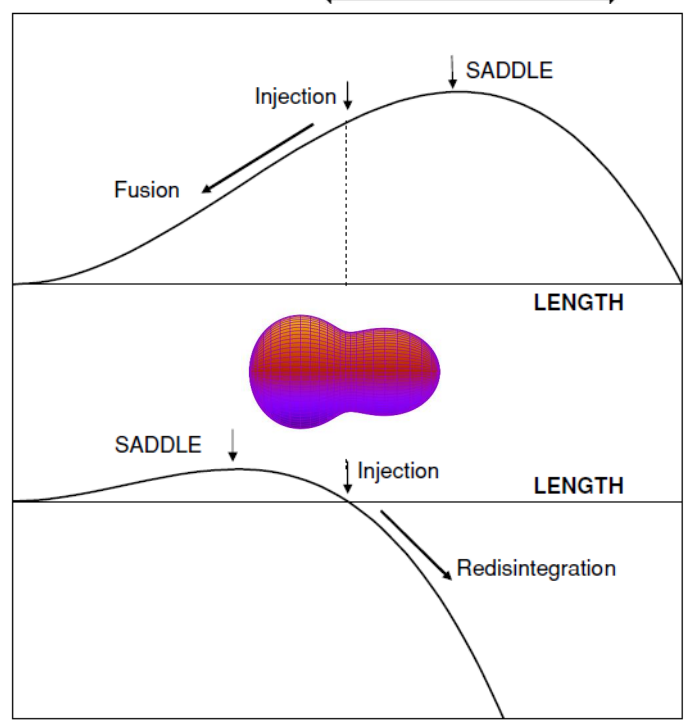


Scission point
symmetrical fission

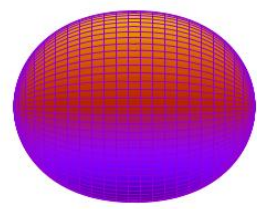
Fusion starting points
(injection point)
 $^{51}\text{V} + ^{248}\text{Cm} \rightarrow ^{299}\text{119}$



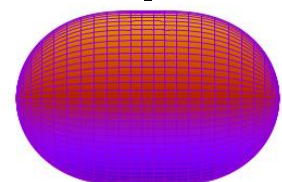
FBD



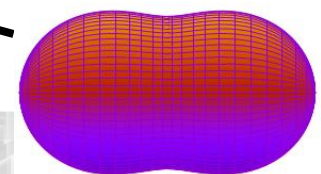
Compound nucleus



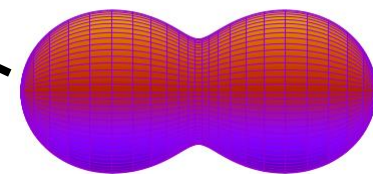
Fission saddle point

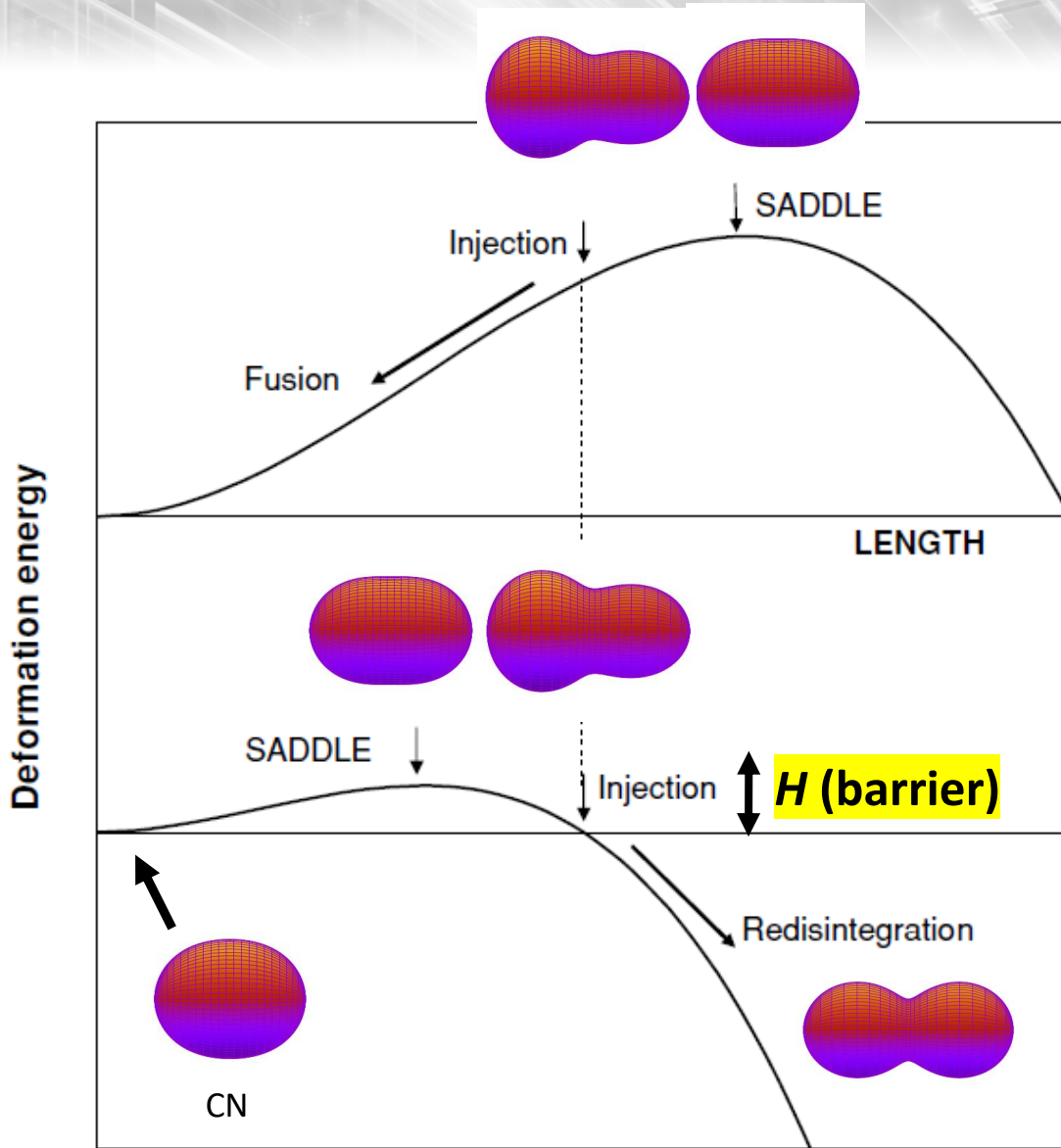


2nd minimum



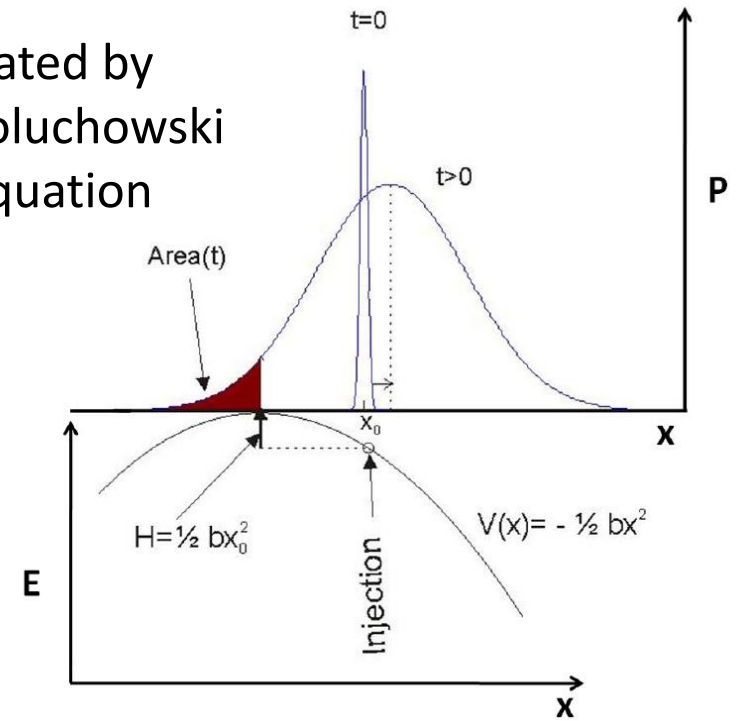
Scission point
symmetric fission





L is the effective elongation (along the fusion path)

P_{fus} is calculated by solving 1D Smoluchowski Diffusion Equation

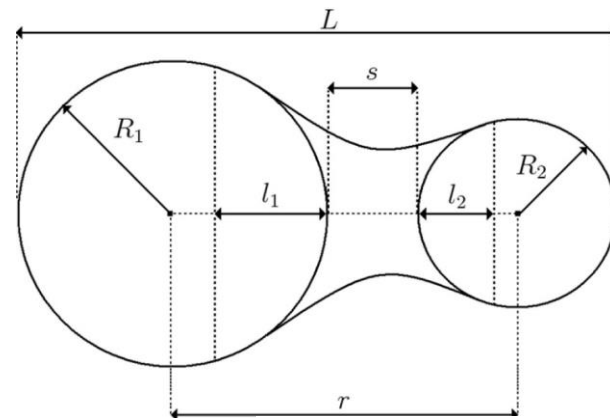
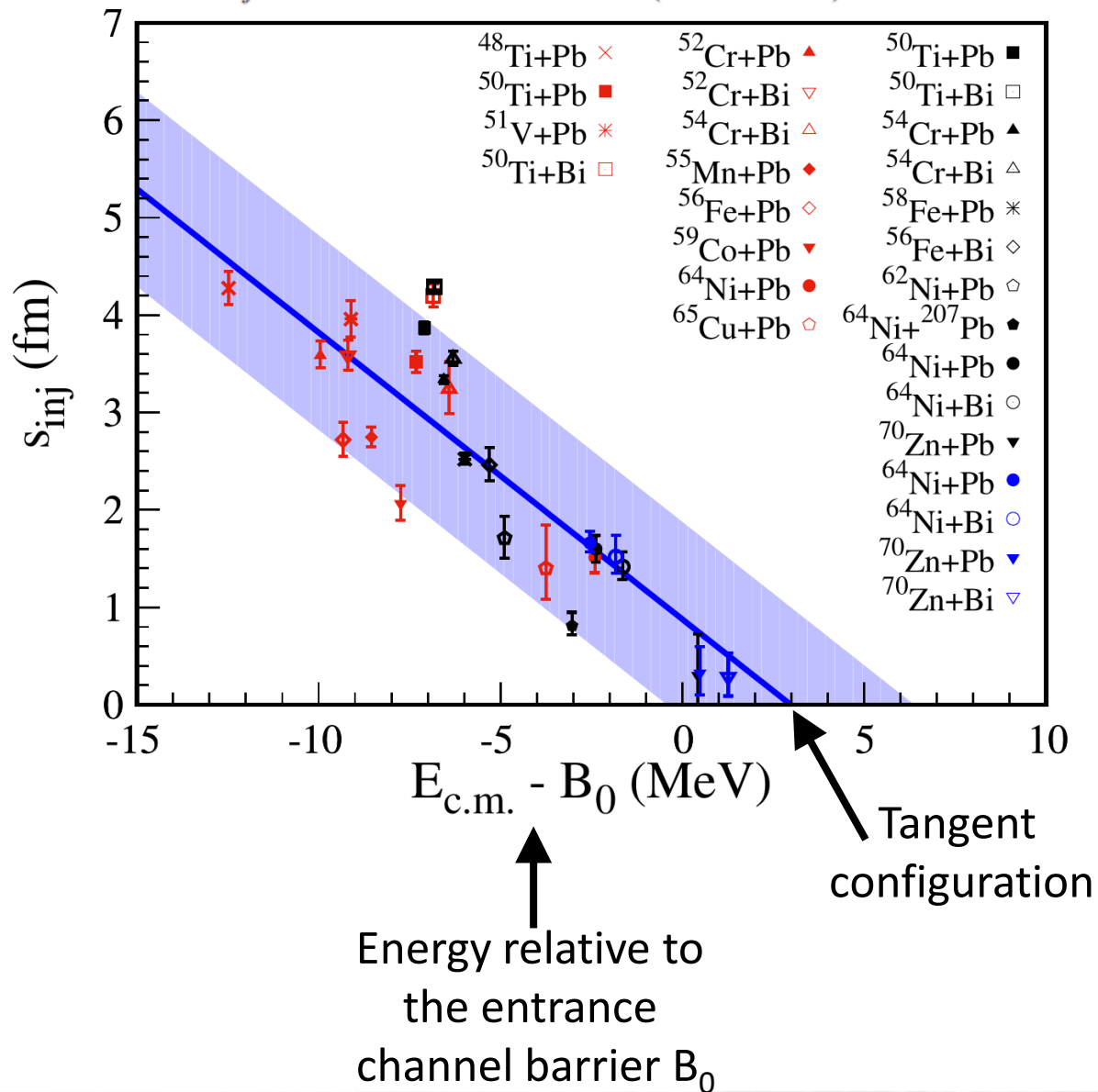


$$P_{fus}(l) = \frac{1}{2} \begin{cases} 1 + \operatorname{erf} \sqrt{\frac{H(l)}{T}} & : L_{inj} < L_{sp} \\ 1 - \operatorname{erf} \sqrt{\frac{H(l)}{T}} & : L_{inj} \geq L_{sp} \end{cases}$$

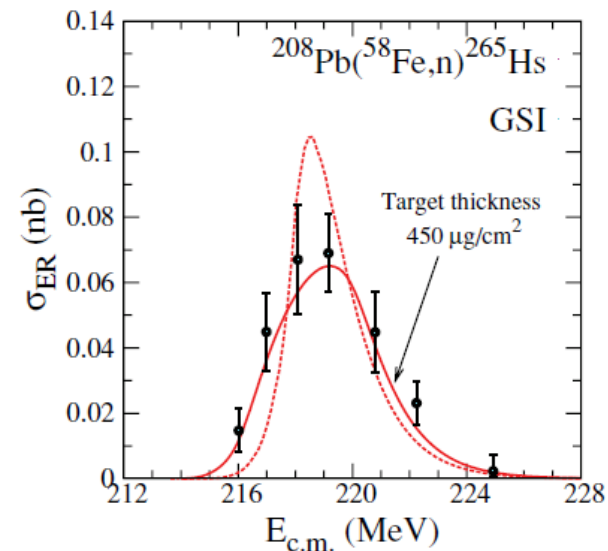
$H(l)$ – the function of angular momentum and bombarding energy

T – the temperature depends on available energy

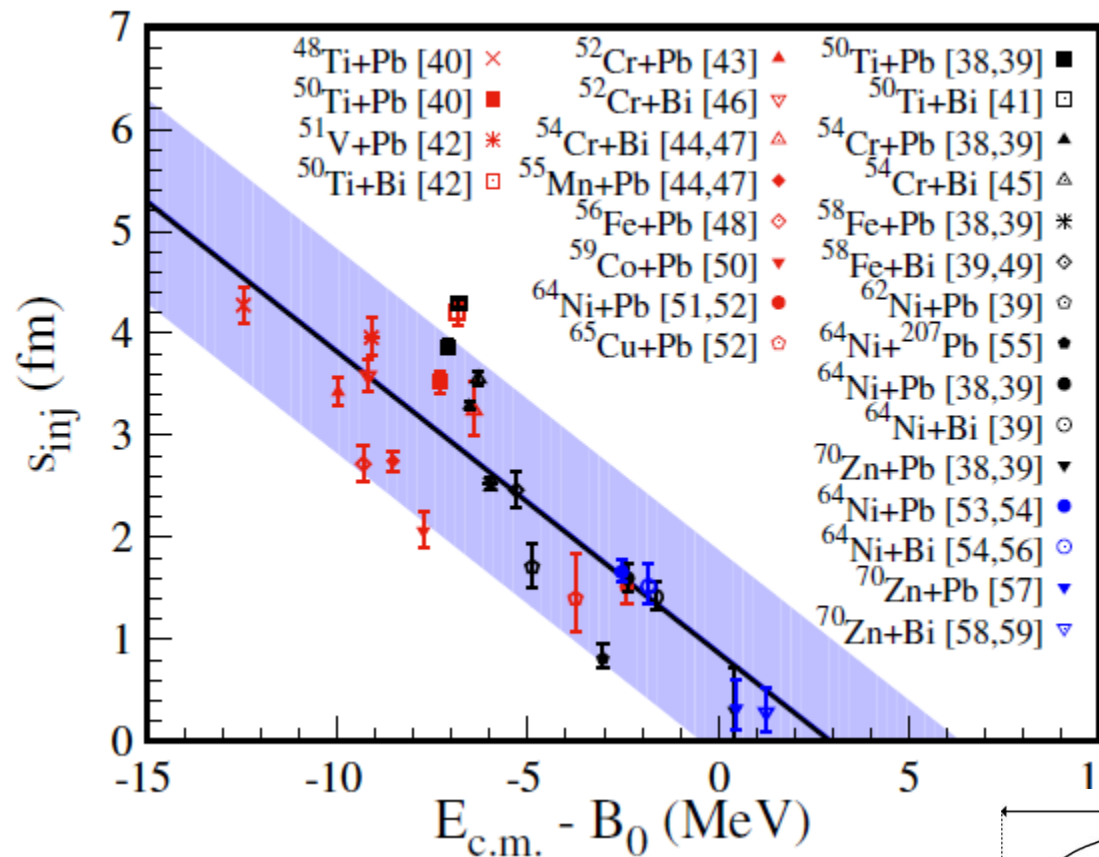
$$s_{inj} = 0.878 \text{ fm} - 0.294 \times (E_{c.m.} - B_0) \text{ fm/MeV}$$



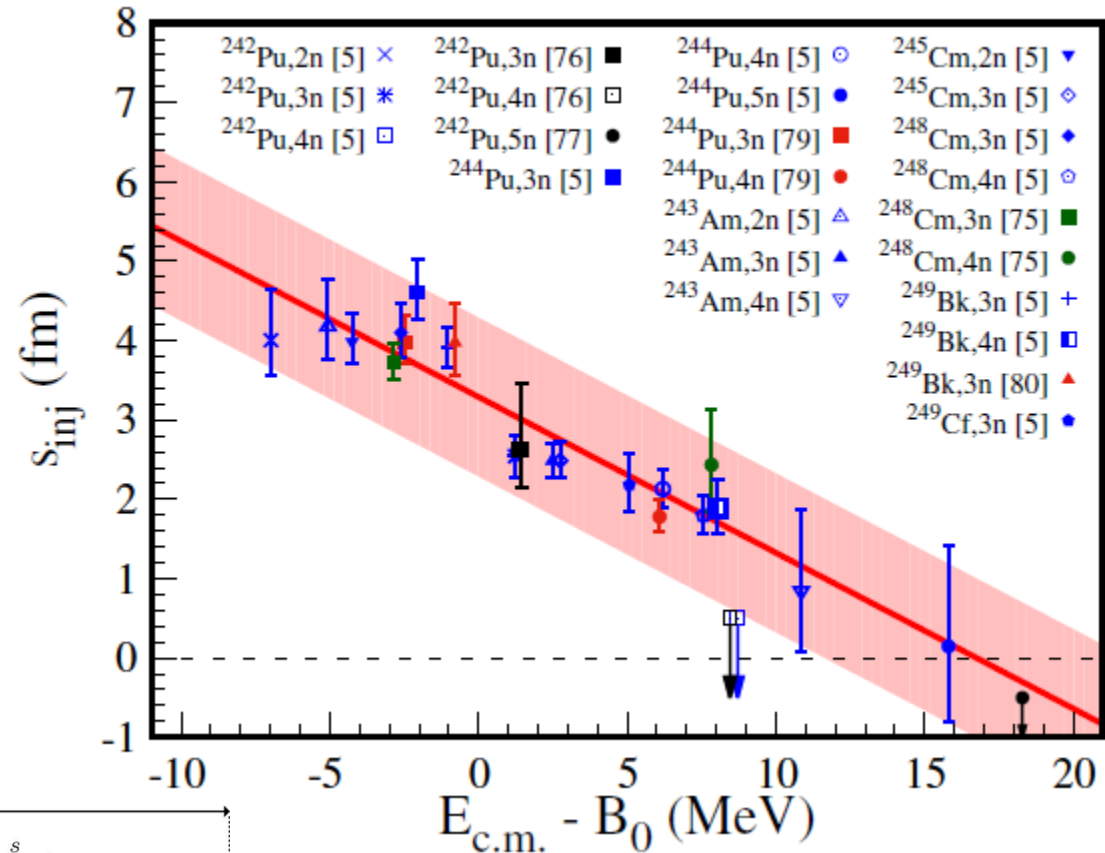
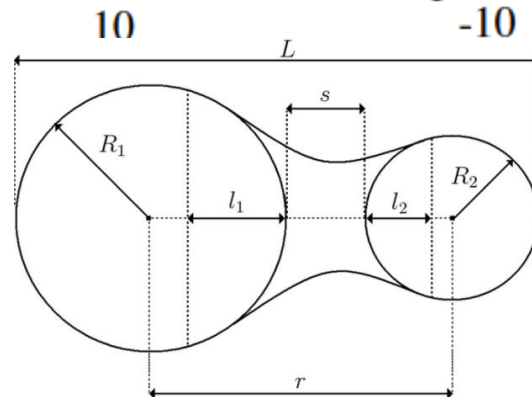
The distance between the nuclear surfaces of two colliding nuclei at the injection point s_{inj} is the only adjustable parameter of the model.



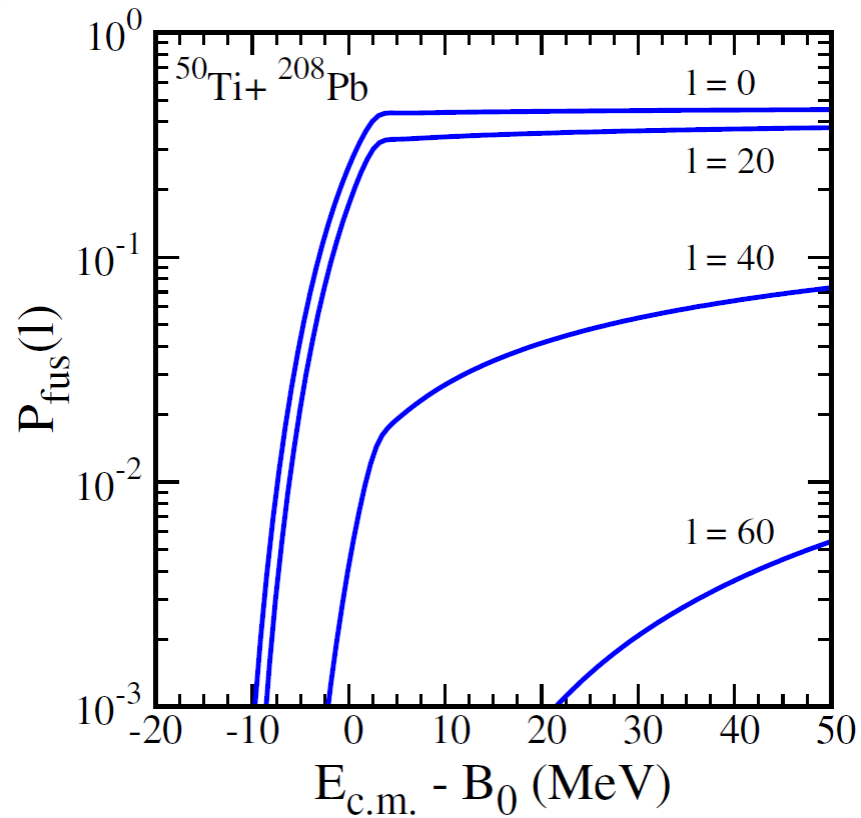
s_{inj} distance was parametrized by analyzing 27 cold fusion reactions.



$$s_{\text{inj}} = 0.878 \text{ fm} - 0.294 \times (E_{\text{c.m.}} - B_0) \text{ fm/MeV}$$



$$s_{\text{inj}} = 3.291 \text{ fm} - 0.196 \times (E_{\text{c.m.}} - B_0) \text{ fm/MeV}$$

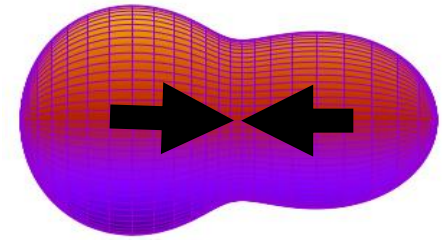


Energy relative to the entrance channel barrier B_0

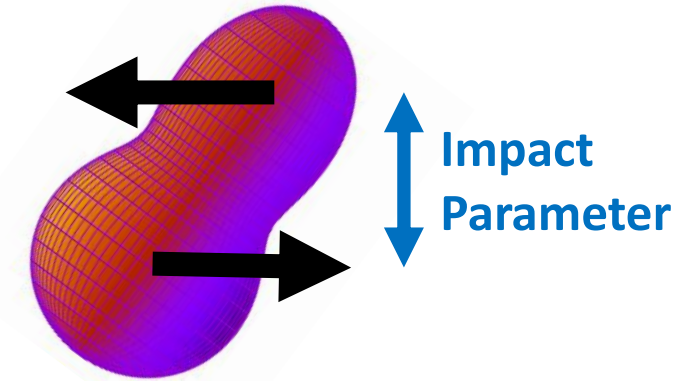
Fusion probability averaged over l

$$\langle P_{\text{fus}} \rangle = \frac{1}{(l_{\text{max}} + 1)^2} \sum_{l=0}^{l_{\text{max}}} (2l + 1) \times P_{\text{fus}}(l)$$

$l = 0$
Central collision

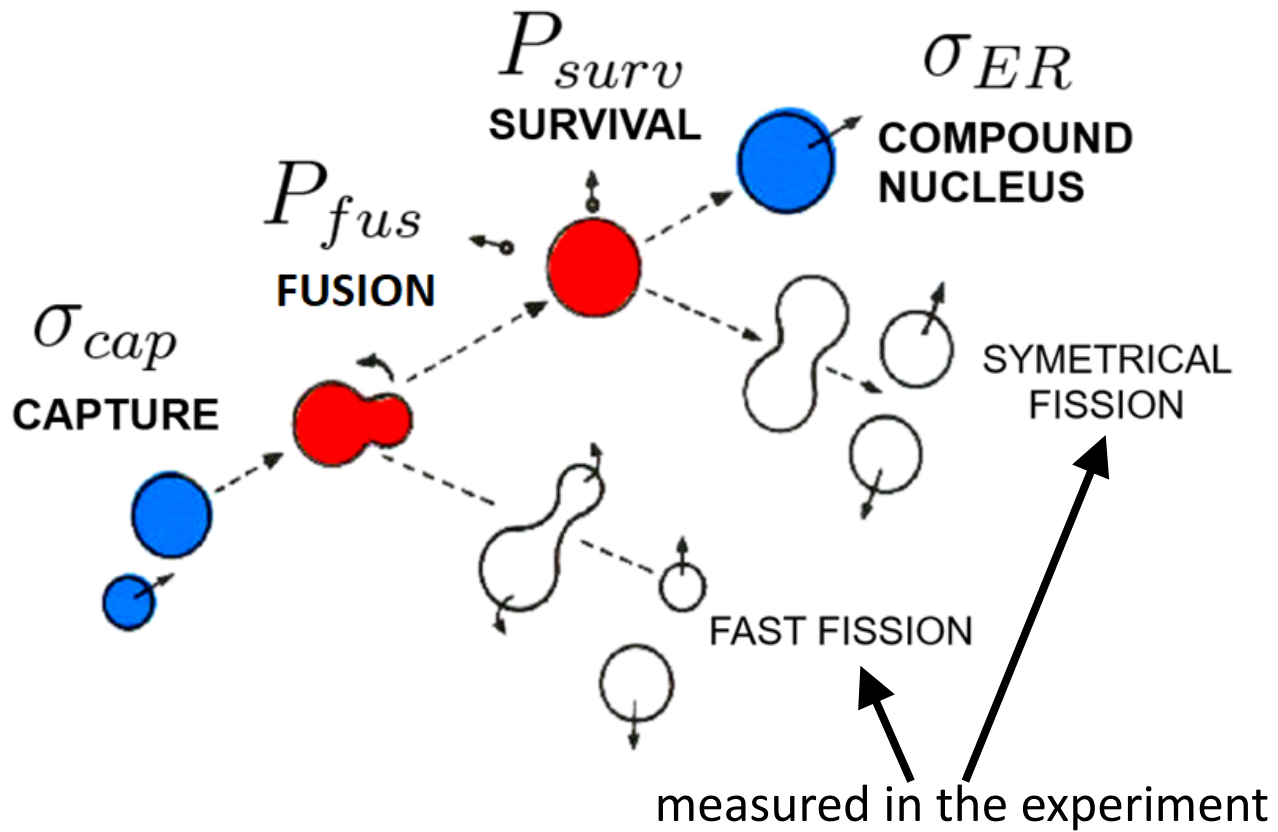


Peripheral collisions



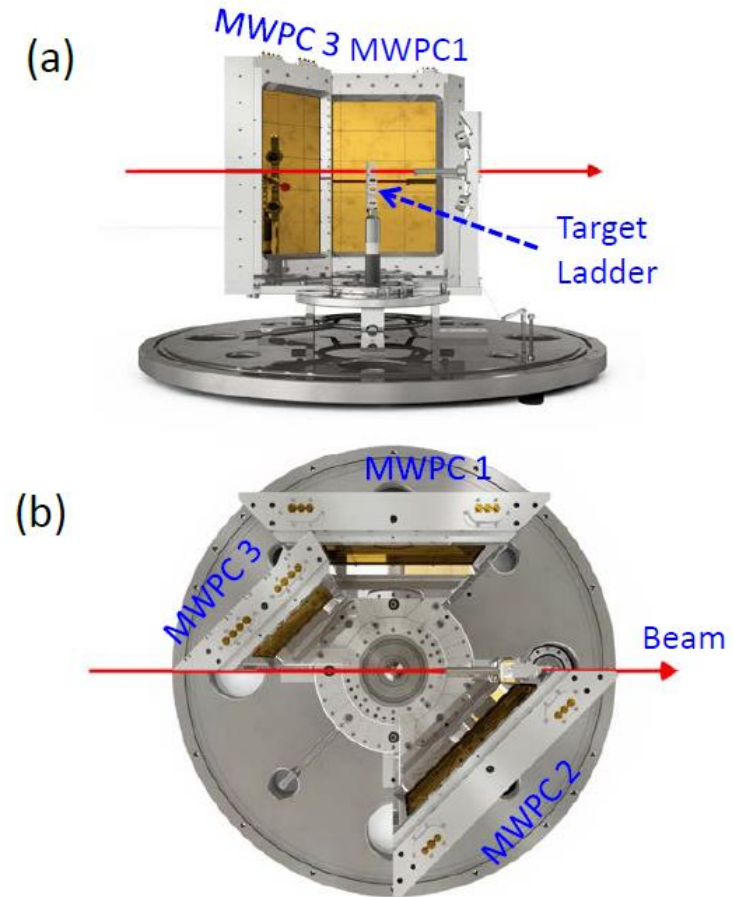
Higher partial waves l
= Higher rotational energy
= Higher barrier $H(l)$
= Lower $P_{\text{fus}}(l)$

Reactions: ^{48}Ca , ^{50}Ti , ^{54}Cr + ^{208}Pb



Mechanisms Suppressing Superheavy Element Yields in Cold Fusion Reactions

Banerjee *et al.*, PRL 122, 232503 (2019)



Review [Progress in Particle and Nuclear Physics 118 \(2021\) 103856](#)

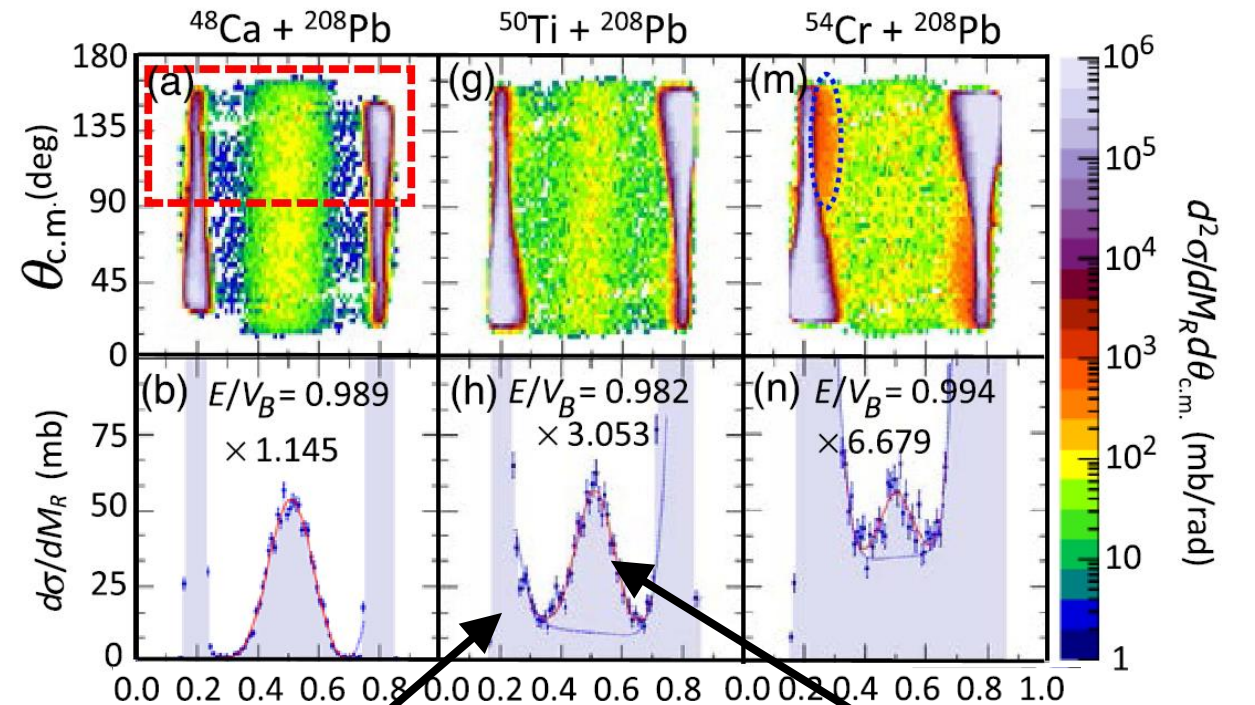
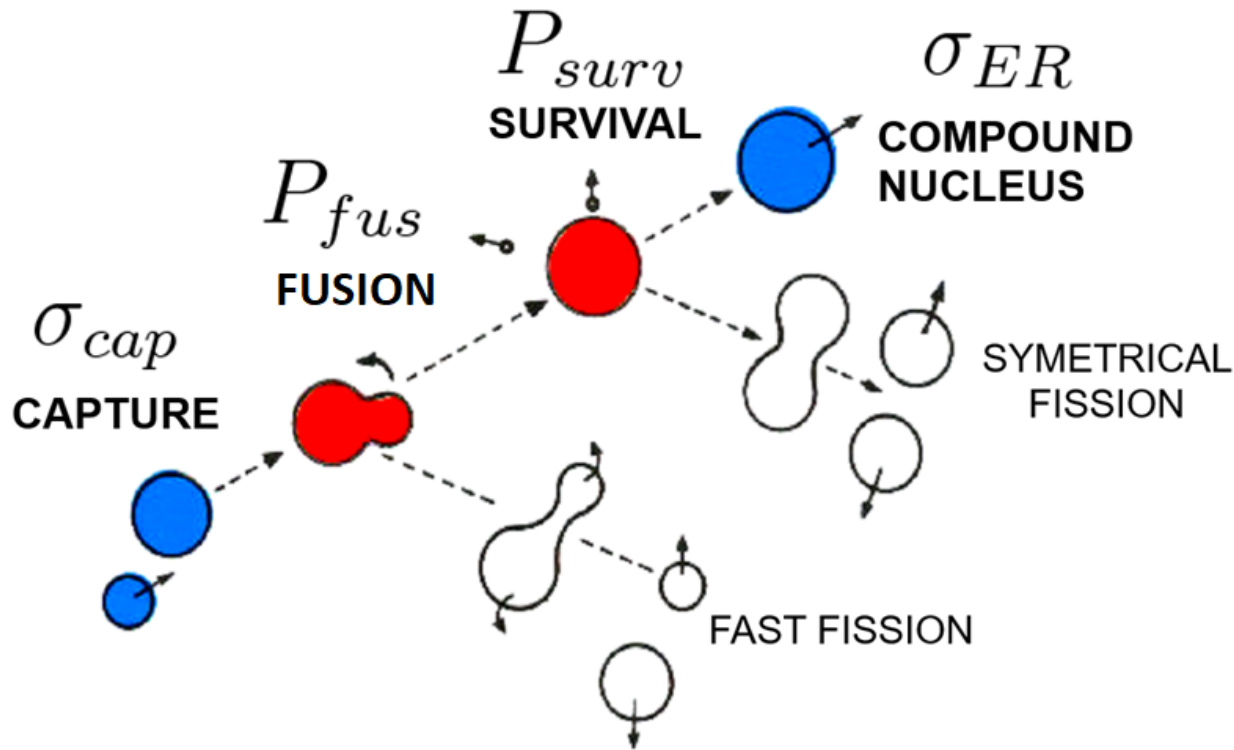
Experimental studies of the competition between fusion and quasifission in the formation of heavy and superheavy nuclei

D.J. Hinde*, M. Dasgupta, E.C. Simpson

Department of Nuclear Physics, Research School of Physics, Australian National University, ACT 2601, Australia

Mechanisms Suppressing Superheavy Element Yields in Cold Fusion Reactions

Banerjee *et al.*, PRL 122, 232503 (2019)



P_{fus} can be experimentally estimated:

$$P_{sym} = \frac{\text{Fusion-Fission cross section}}{\text{Capture cross section}}$$

Fast Fission cross section

Mass ratio, symmetric split: $M_R = 0.5$

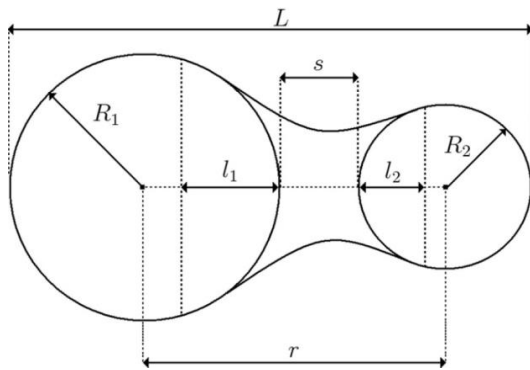
Fusion-Fission cross section (symmetrical fission)

Fusion probability averaged over l

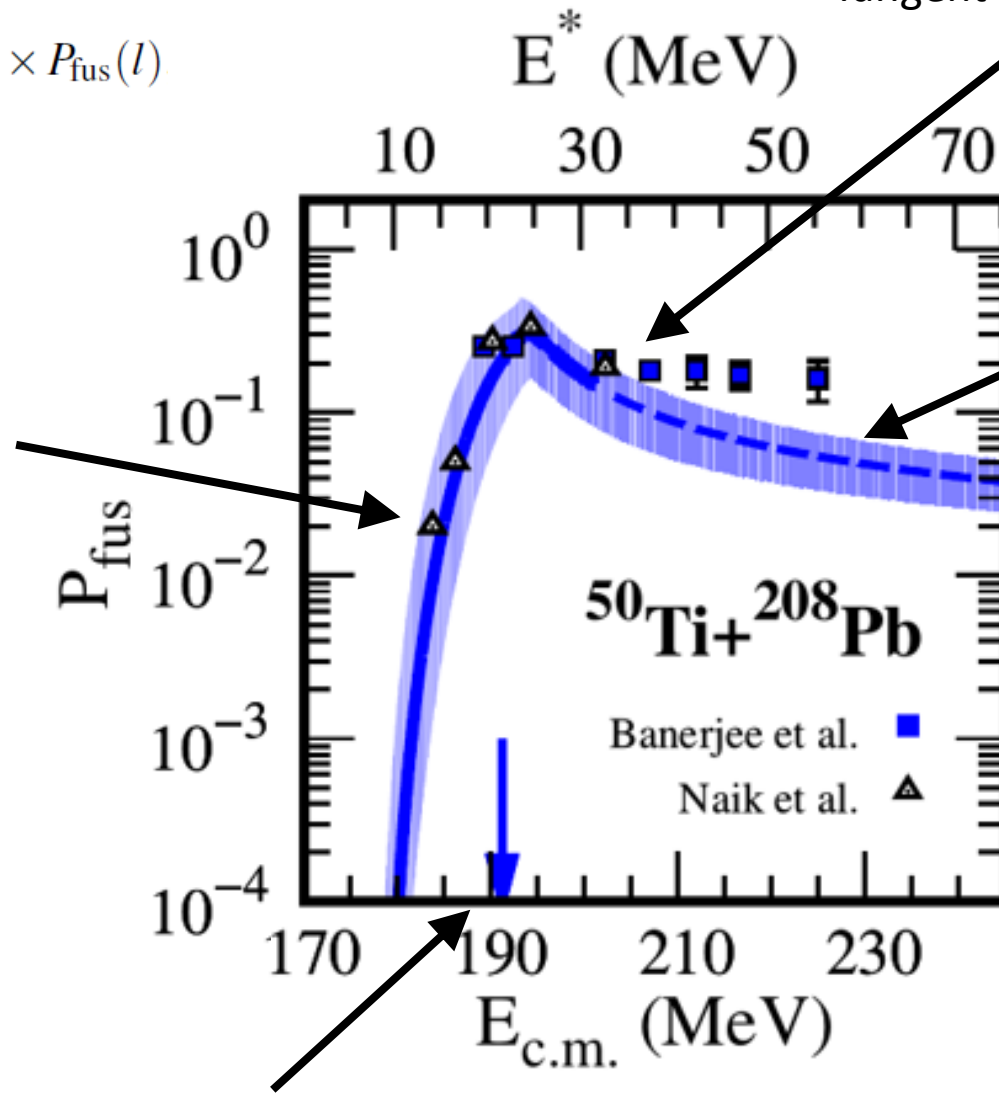
$$\langle P_{\text{fus}} \rangle = \frac{1}{(l_{\text{max}} + 1)^2} \sum_{l=0}^{l_{\text{max}}} (2l + 1) \times P_{\text{fus}}(l)$$

Below B_0 , the $\langle P_{\text{fus}} \rangle$ growth comes from the reduction in the height of the internal barrier opposing fusion.

$s_{\text{injection}} > 0 \text{ fm}$



Tangent configuration of projectile and target
($s_{\text{injection}} = 0 \text{ fm}$)



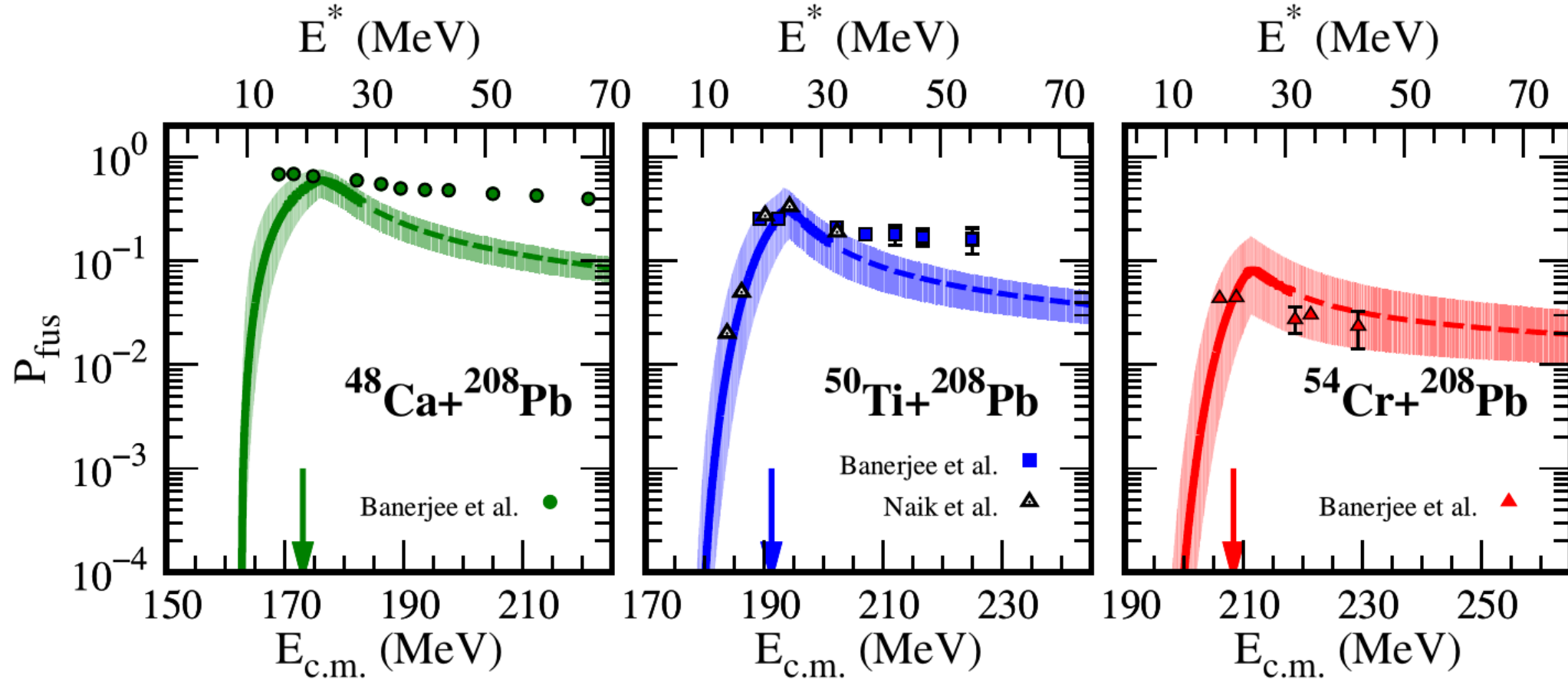
The $\langle P_{\text{fus}} \rangle$ saturation above B_0 results from suppression of the contributions from higher partial waves and can be linked to the critical angular momentum.

The difference between rotational energies in the fusion saddle and the contact (sticking) configuration plays a major role in CN formation at energies above B_0 .

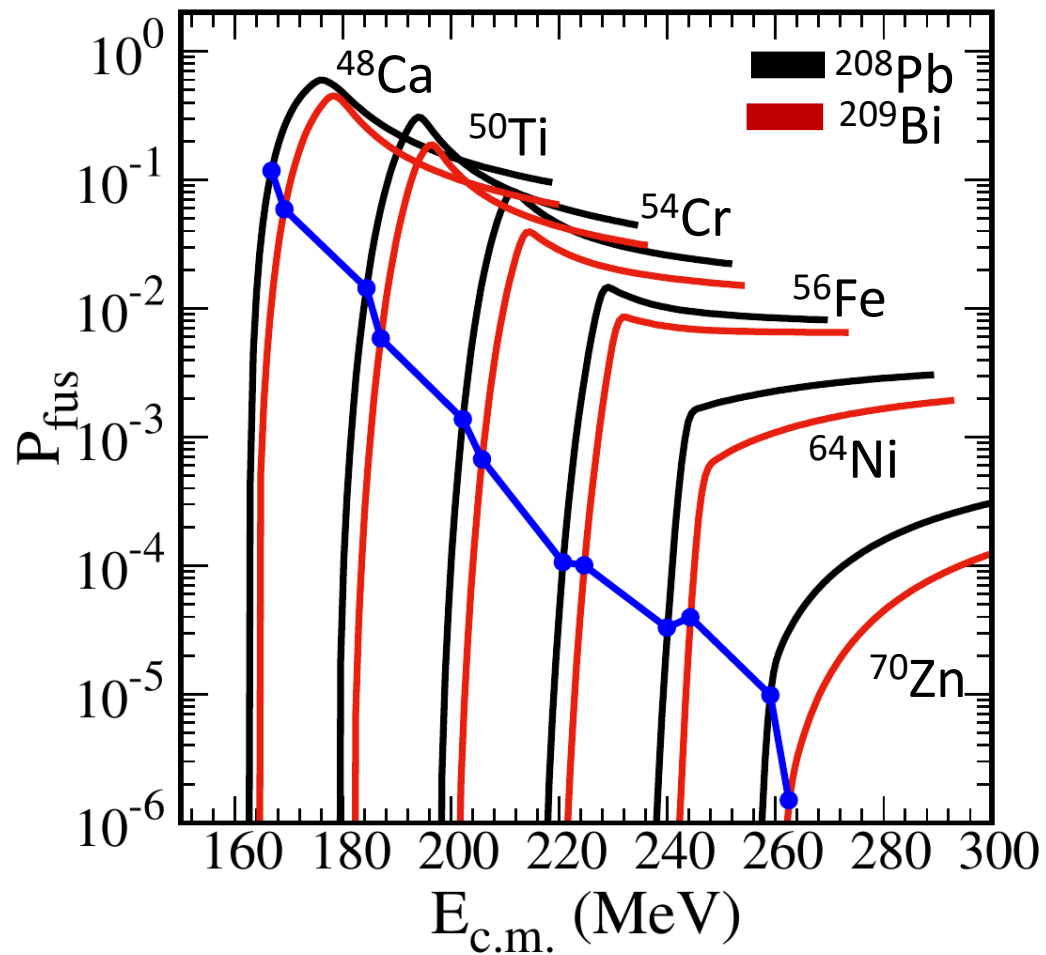
B_0 - entrance channel barrier (Coulomb + Nuclear potential)

Fusion probability averaged over l

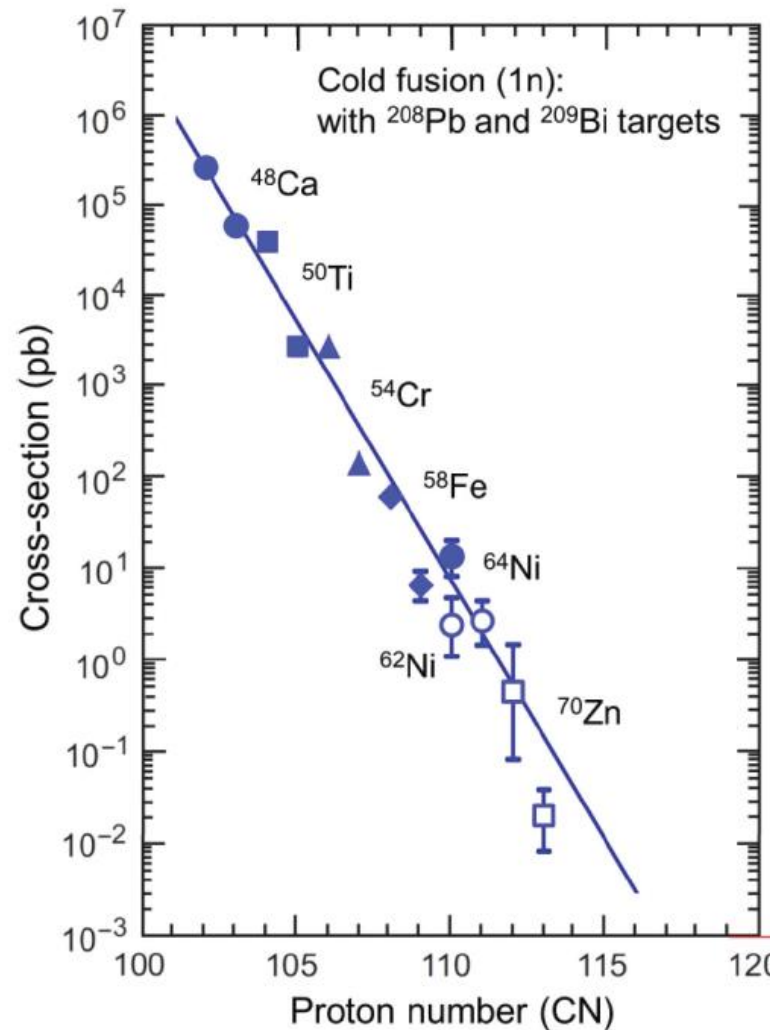
$$\langle P_{\text{fus}} \rangle = \frac{1}{(l_{\text{max}} + 1)^2} \sum_{l=0}^{l_{\text{max}}} (2l + 1) \times P_{\text{fus}}(l)$$



Diffusion as a possible mechanism controlling the production of superheavy nuclei in cold fusion reactions



Blue line – P_{fus} at the predicted optimal bombarding energies for the $1n$ channel



The Fusion-by-Diffusion model as a tool to calculate cross sections for the production of superheavy nuclei

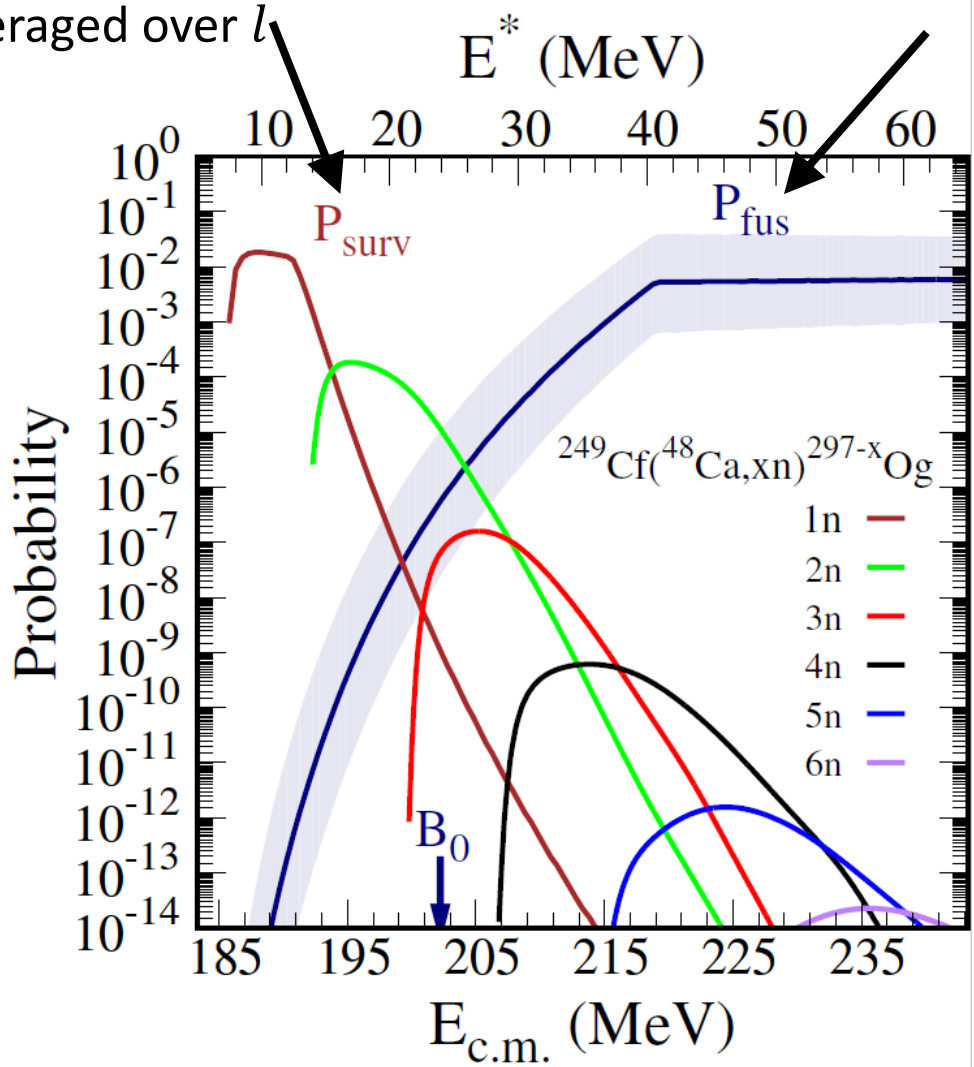
T. Cap^{a,1}, M. Kowal^{b,1}, K. Siwek-Wilczyńska^{c,2}

Eur. Phys. J. A (2022) 58:231

$$\langle P_{\text{surv}} \rangle = \frac{1}{(l_{\text{max}} + 1)^2} \sum_{l=0}^{l_{\text{max}}} (2l + 1) \times P_{\text{surv}}(l)$$

Survival probability averaged over l

Fusion probability averaged over l



For hot Fusion reactions

P_{surv} is calculated using Monte Carlo methods:

$$P_{\text{surv}}^{\text{xn}}(l) = \prod_{i=1}^x \left(\frac{\Gamma_n}{\Gamma_n + \Gamma_f} \right)_i \times P_{<}$$

Competition between **neutron emission** and **fission**

Weisskopf formula

$$\Gamma_n = \frac{g m_n \sigma_n}{\pi^2 \hbar^2 \rho_{\text{G.S.}}} \int_0^{X_n} \rho_n(X_n - \epsilon_n) \epsilon_n d\epsilon_n$$

$$X_n = E^* - B_n - E_{\text{rot}}^{A-1}(l)$$

$$X_f = E^* - B_f - E_{\text{rot}}^{\text{sp}}(l)$$

$$\Gamma_f = \frac{1}{2\pi \rho_{\text{G.S.}}} \int_0^{X_f} \rho_f(X_f - \epsilon_f) d\epsilon_f$$

Transition-state theory

Properties of heaviest nuclei with $98 \leq Z \leq 126$ and $134 \leq N \leq 192$

P. Jachimowicz^a, M. Kowal^{b,*}, J. Skalski^b

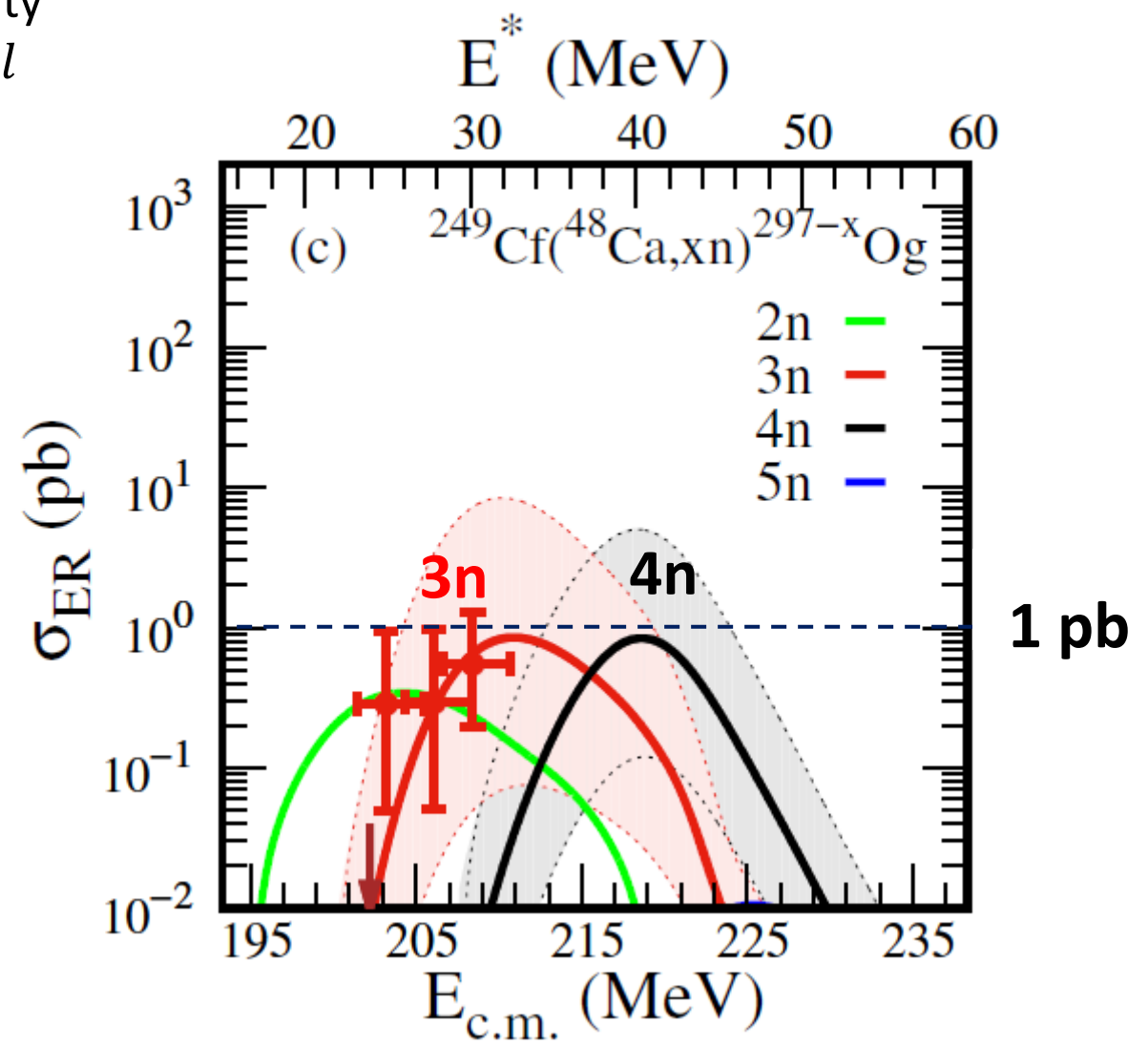
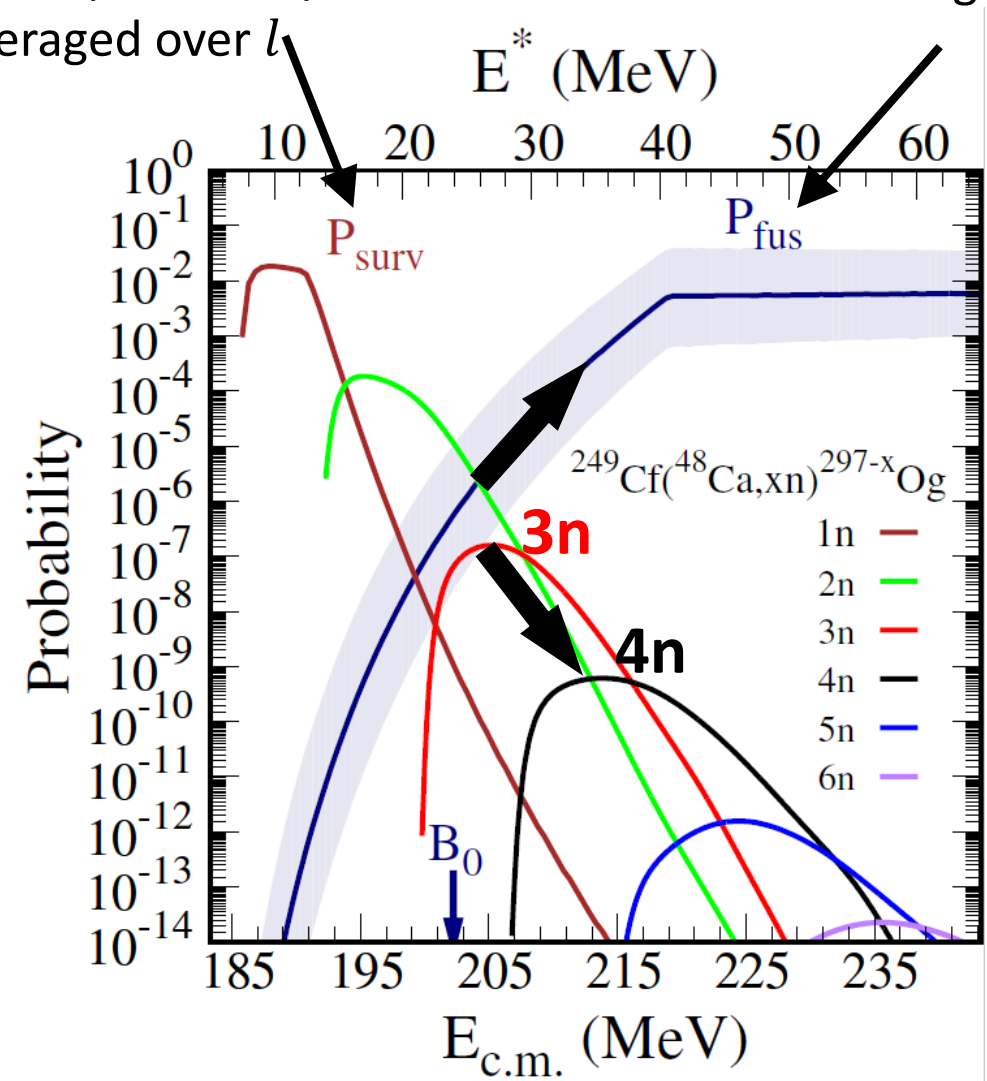
^a Institute of Physics, University of Zielona Góra, Szafrana 4a, 65-516 Zielona Góra, Poland
^b National Centre for Nuclear Research, Pasteura 7, 02-093 Warsaw, Poland

Adiabatic fission barriers

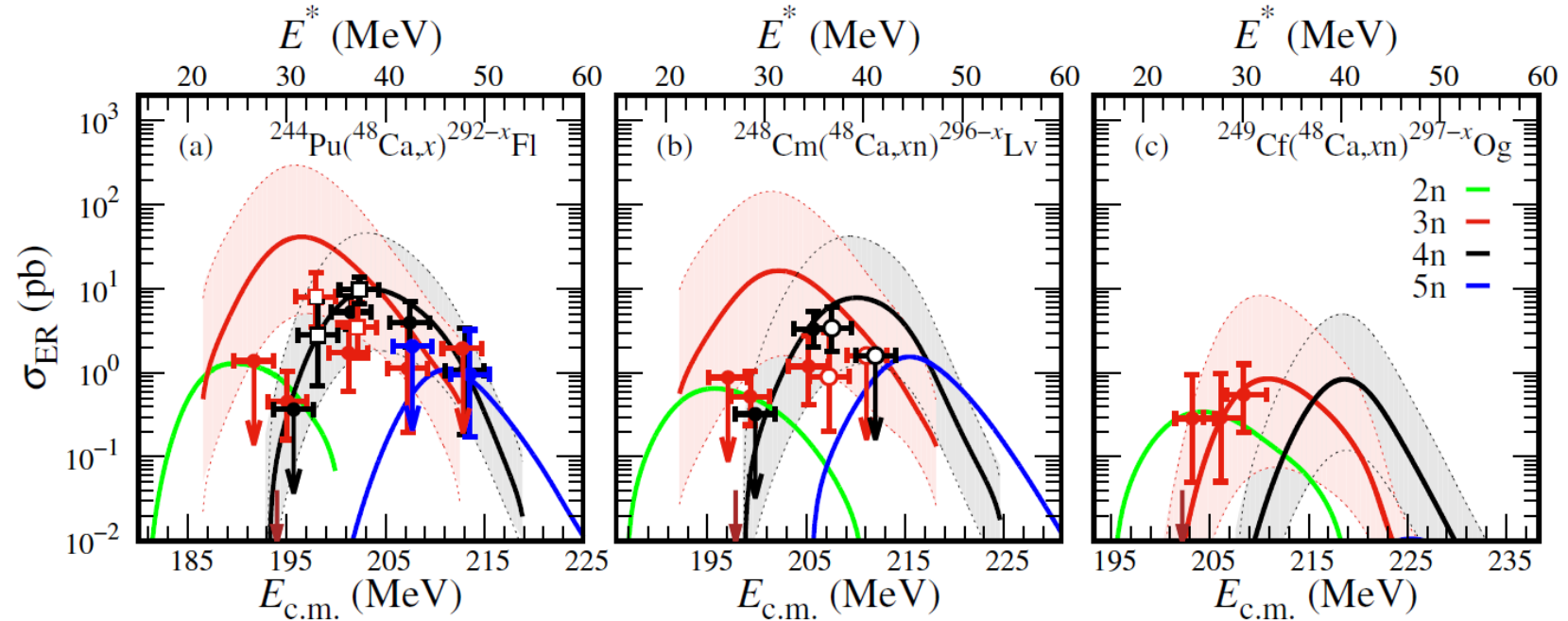
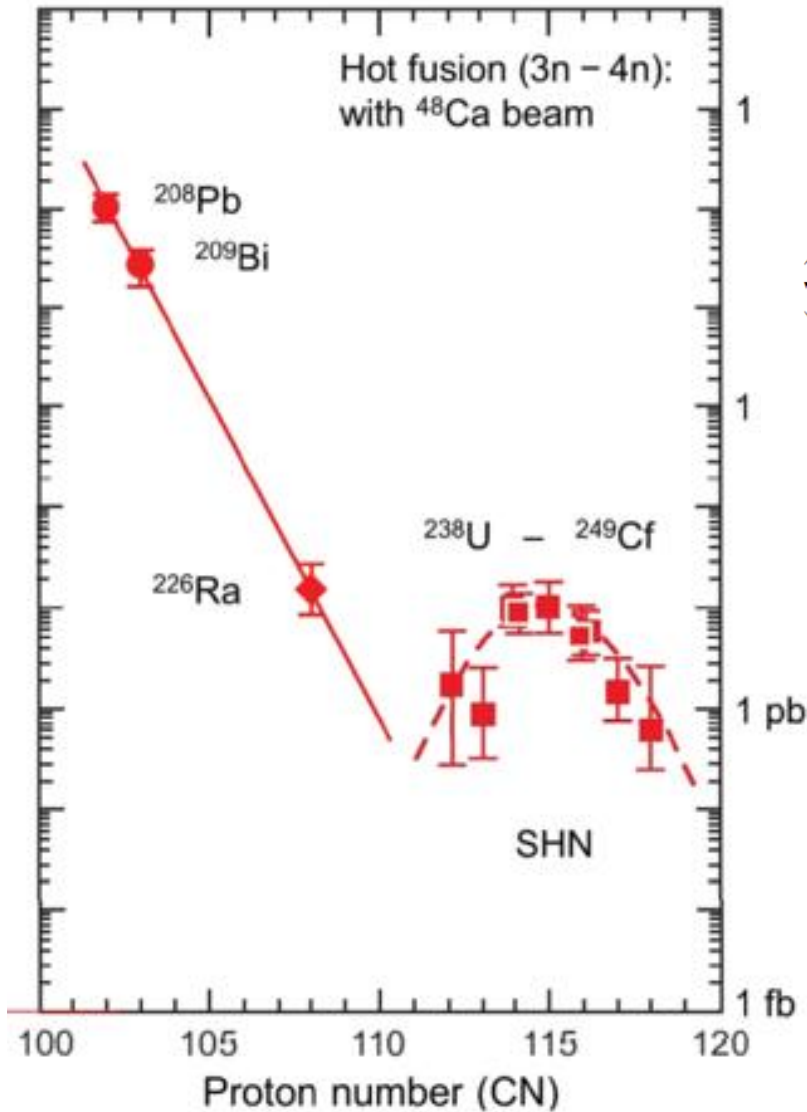
$$\langle P_{\text{surv}} \rangle = \frac{1}{(l_{\text{max}} + 1)^2} \sum_{l=0}^{l_{\text{max}}} (2l + 1) \times P_{\text{surv}}(l)$$

Survival probability averaged over l

Fusion probability averaged over l



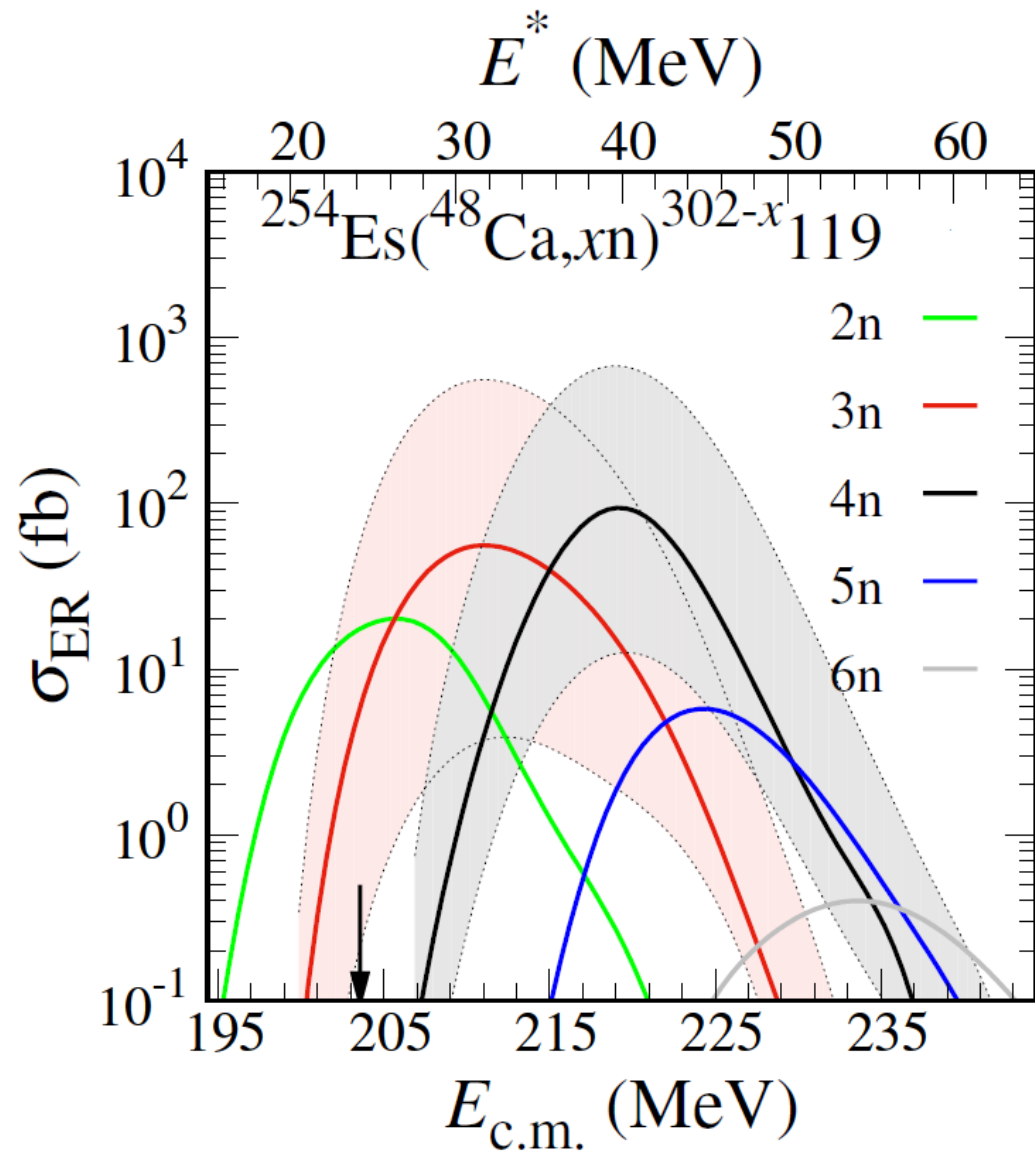
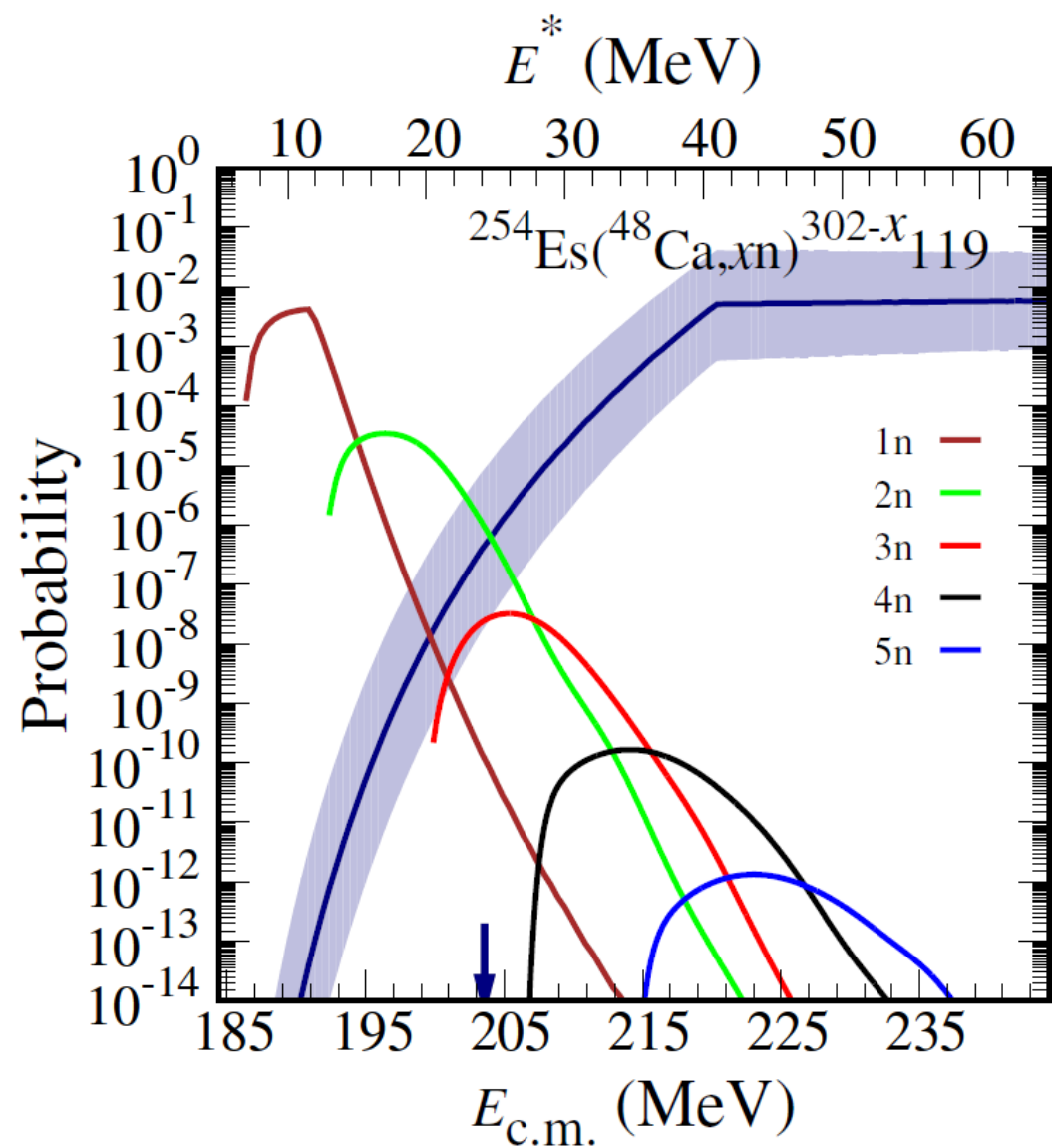
Yu. Ts. Oganessian and V. K. Utyonkov. Rep. Prog. Phys. 78(3):036301, 2015

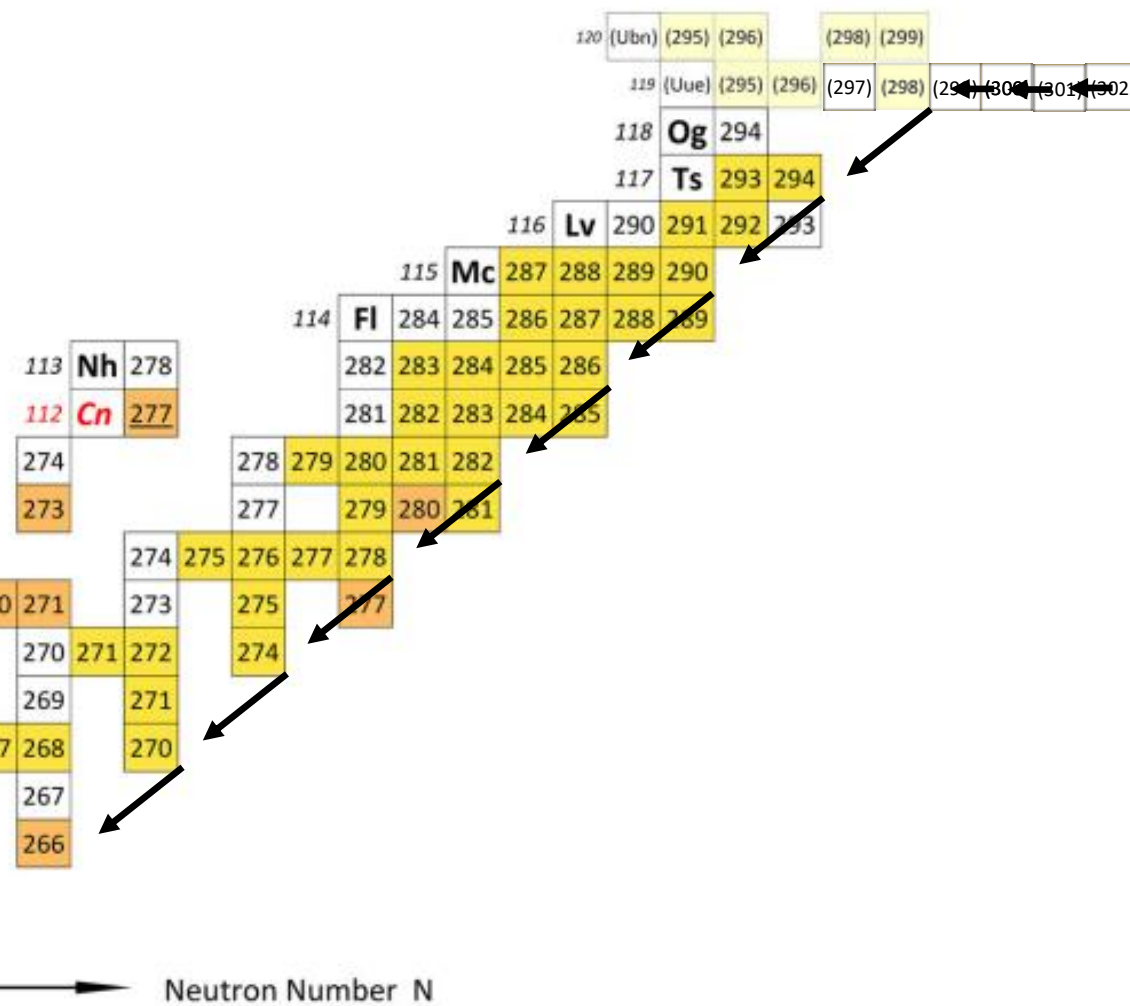
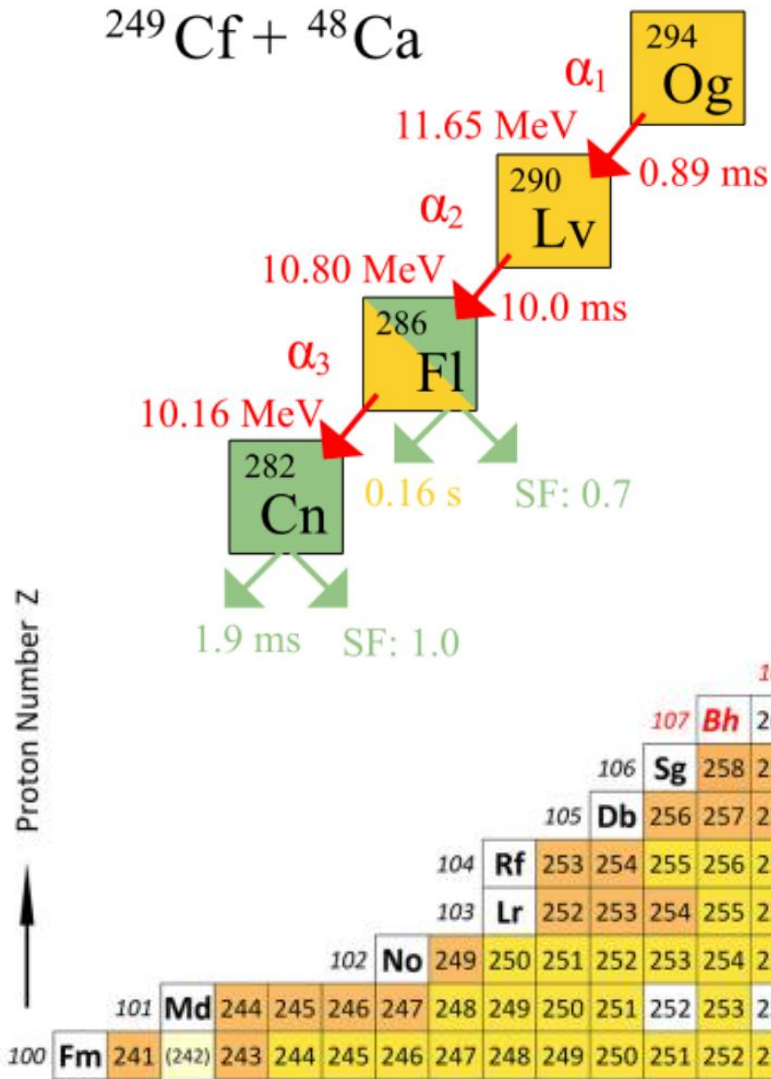
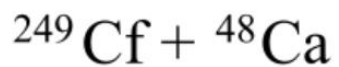
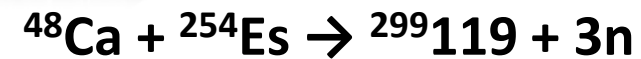


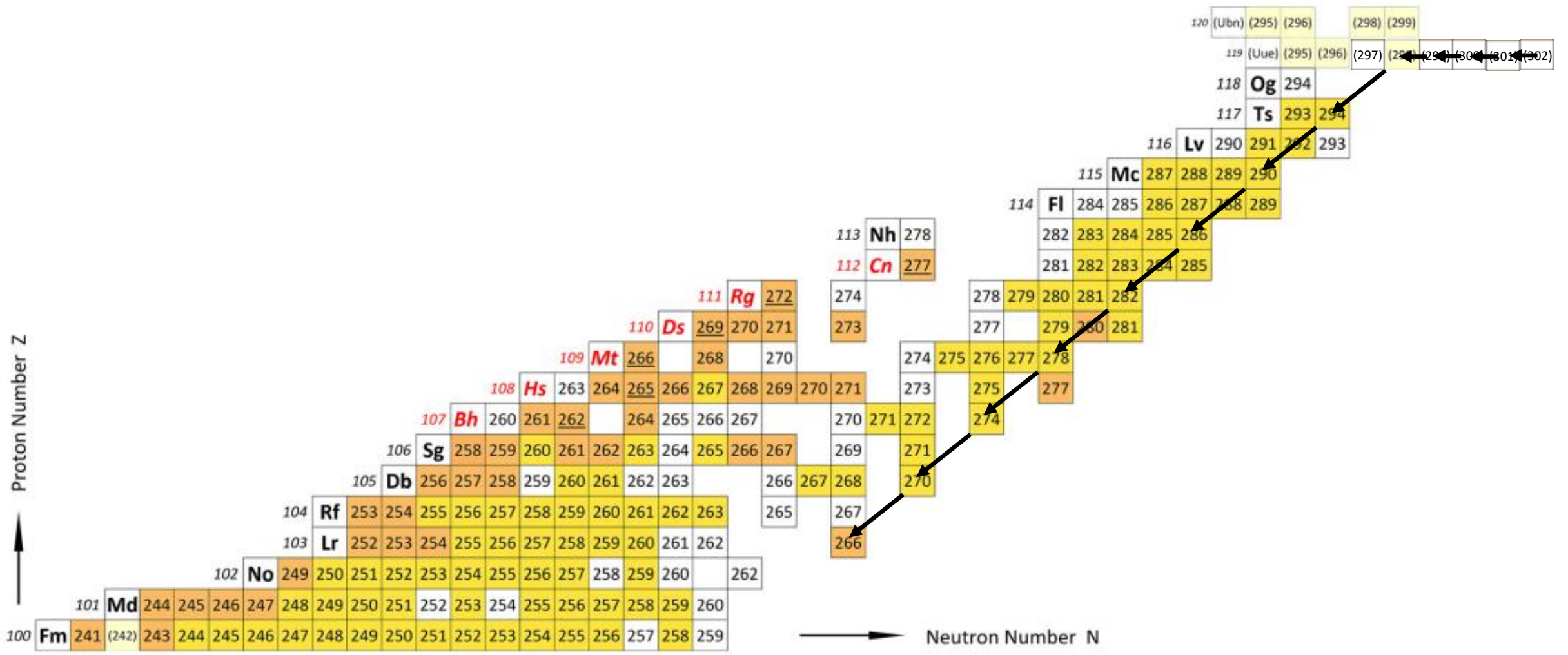
Systematic decrease of the 3n and 4n ER cross sections for the synthesis of the elements 114 – 118 is reproduced in the model.

Is synthesis of elements 119 and 120 possible?
Can we use the same approach for ^{50}Ti and ^{51}V ?

The cross section for $^{48}\text{Ca}+^{254}\text{Es}$ should be around 100 fb.

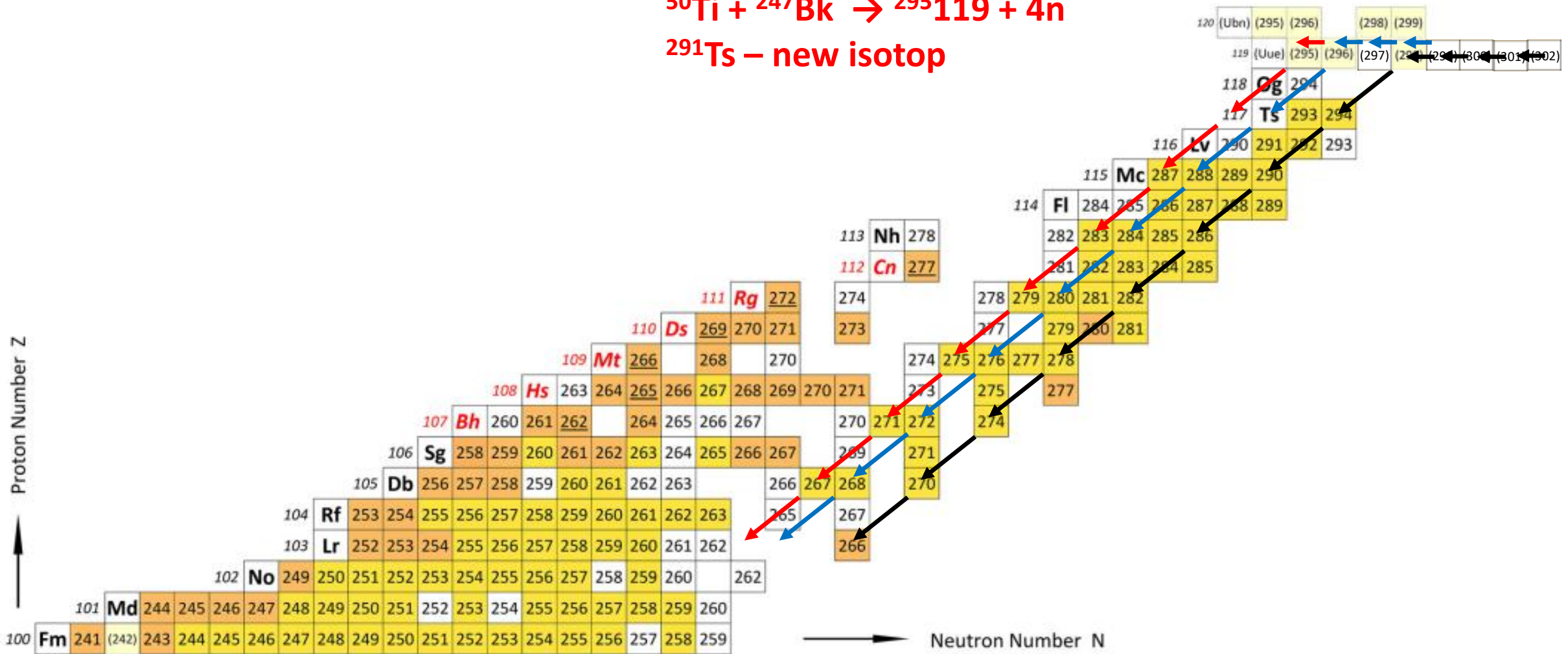






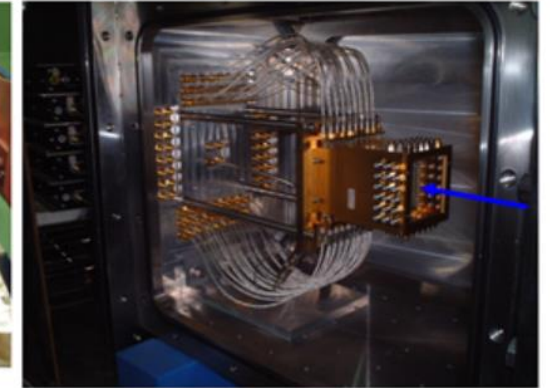
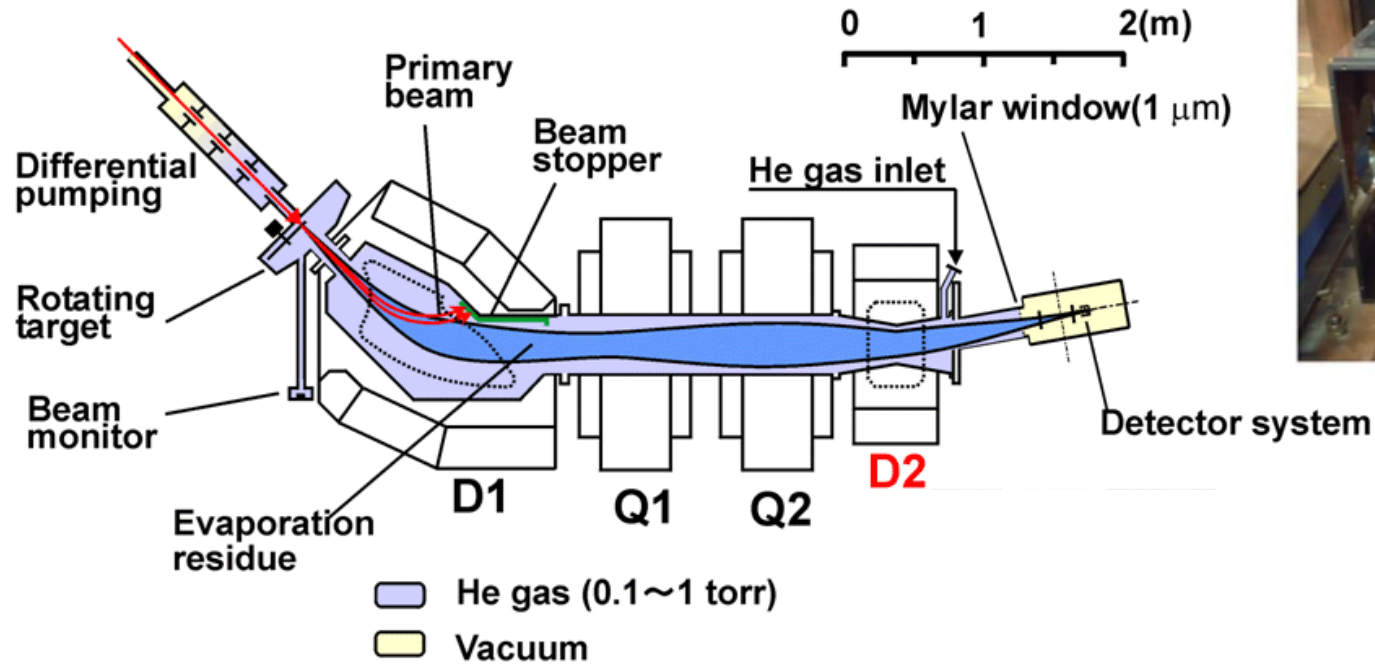


${}^{291}\text{Ts}$ – new isotope

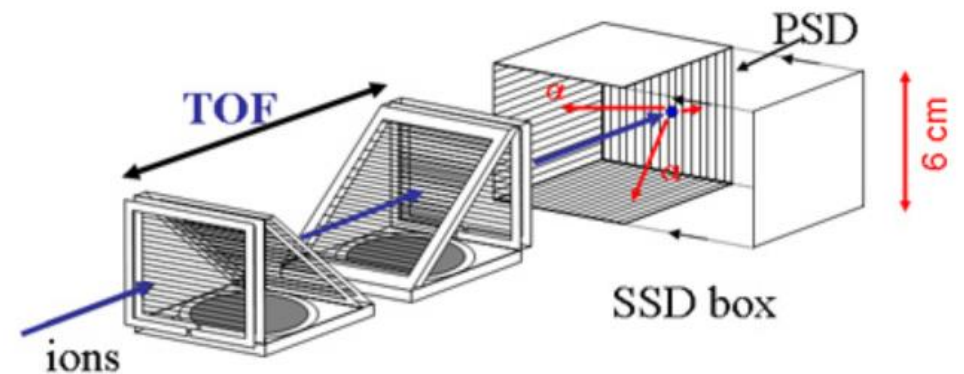


RIKEN GARIS (Gas-filled Recoil Ion Separator)

$^{51}\text{V} + ^{248}\text{Cm}$



Magnification	X	-0.76
	Y	-1.99
Dispersion		0.97 cm/%
Total length		5760 mm
Acceptance	$\Delta\theta$	± 68 mrad
	$\Delta\phi$	± 57 mrad
	$\Delta\Omega$	12.2 msr



Target from ORNL: ^{248}Cm (97%), $500 \mu\text{g}/\text{cm}^2$
 Projectile: ^{51}V , up to $5 \mu\text{A}$
 GARIS transmission: 80%



Figure 13: Assembled TASCA target wheel with four target segments, containing a total amount of about 12 mg ^{249}Bk , deposited by molecular plating on $2\ \mu\text{m}$ Ti backings [144]. The total ^{249}Bk β^- activity was $6 \cdot 10^{11}$ Bq at the beginning of irradiation [86]. (Reprinted by permission from Springer nature Customer Service Centre GmbH: Nature Springer J. Radioanal. Nucl. Chem. 299, 1081–1804 (2014), “Preparation of actinide targets for the synthesis of the heaviest elements”, <https://doi.org/10.1007/s10967-013-2616-6>, J. Runke et al., © 2014).

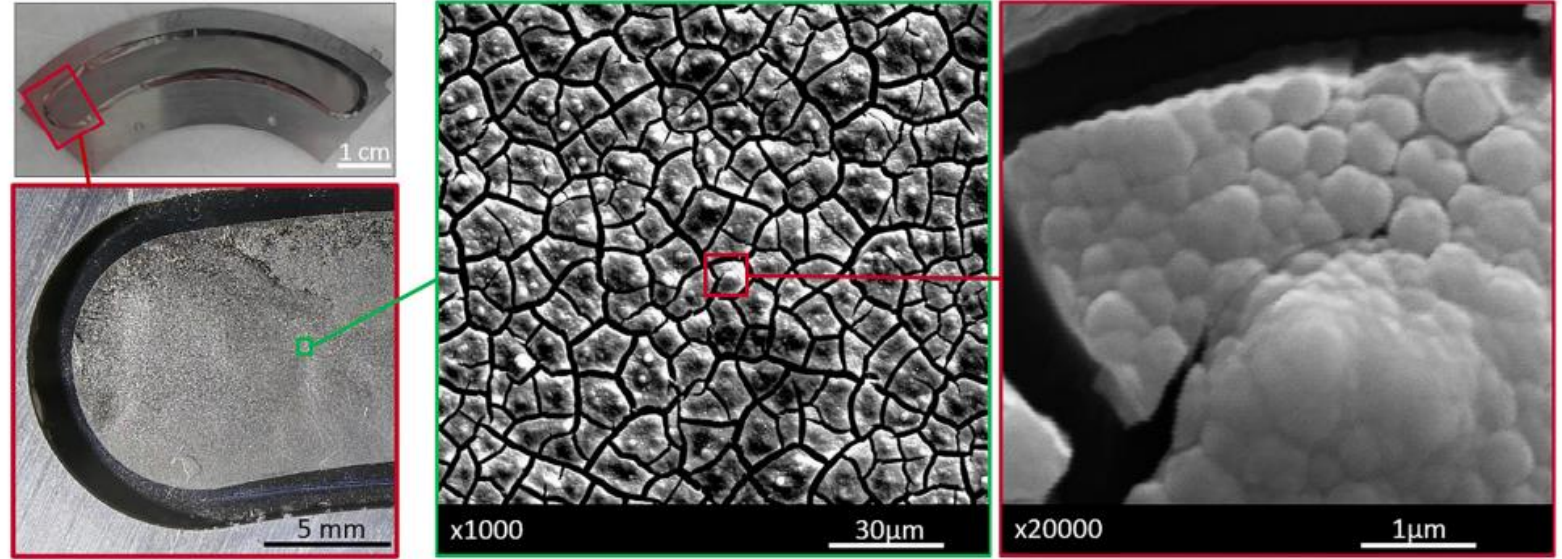


Figure 14: Photographies (top and bottom left) and SEM pictures (center and right) of a $500\ \mu\text{g}/\text{cm}^2$ La target on a TASCA target frame.

FBD model:

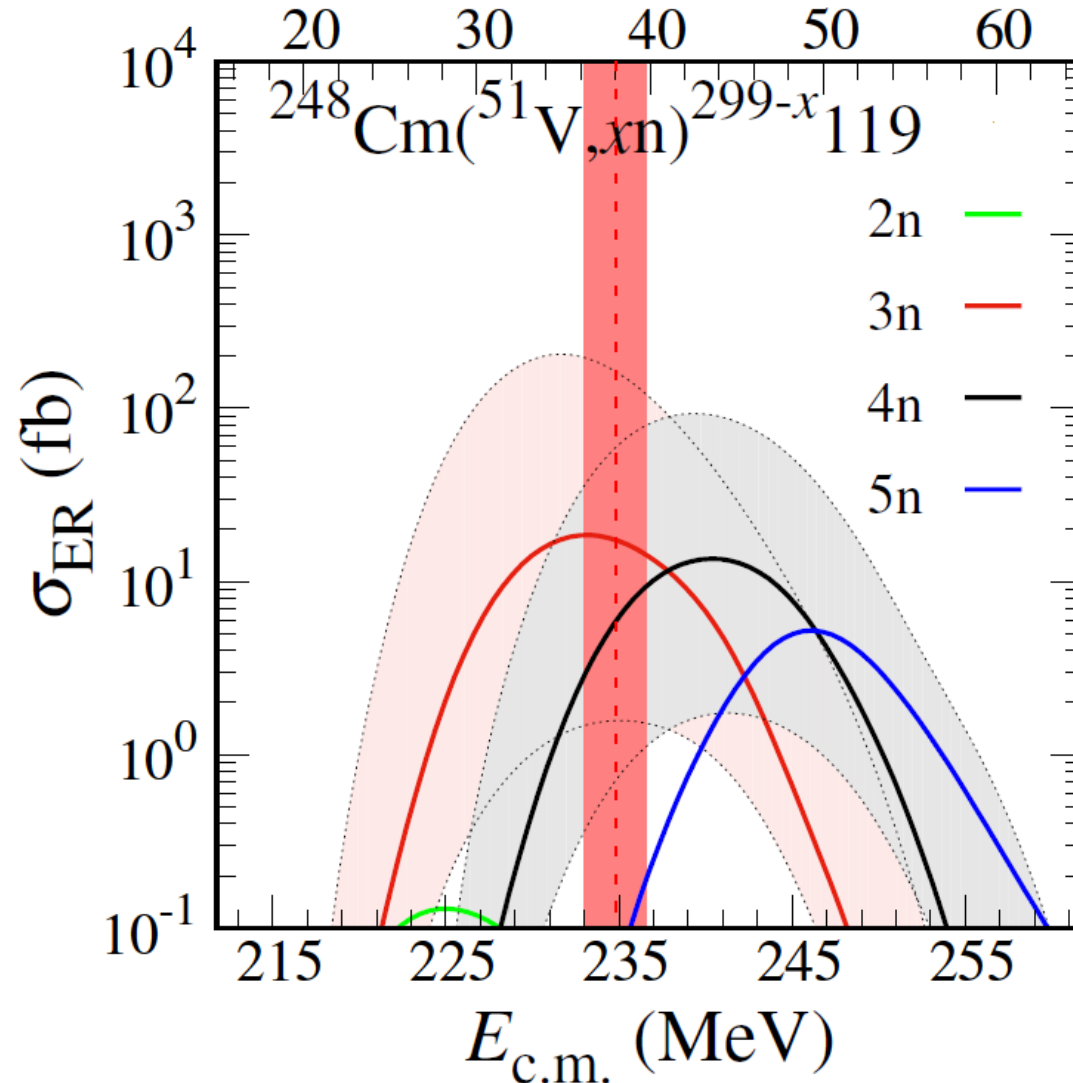
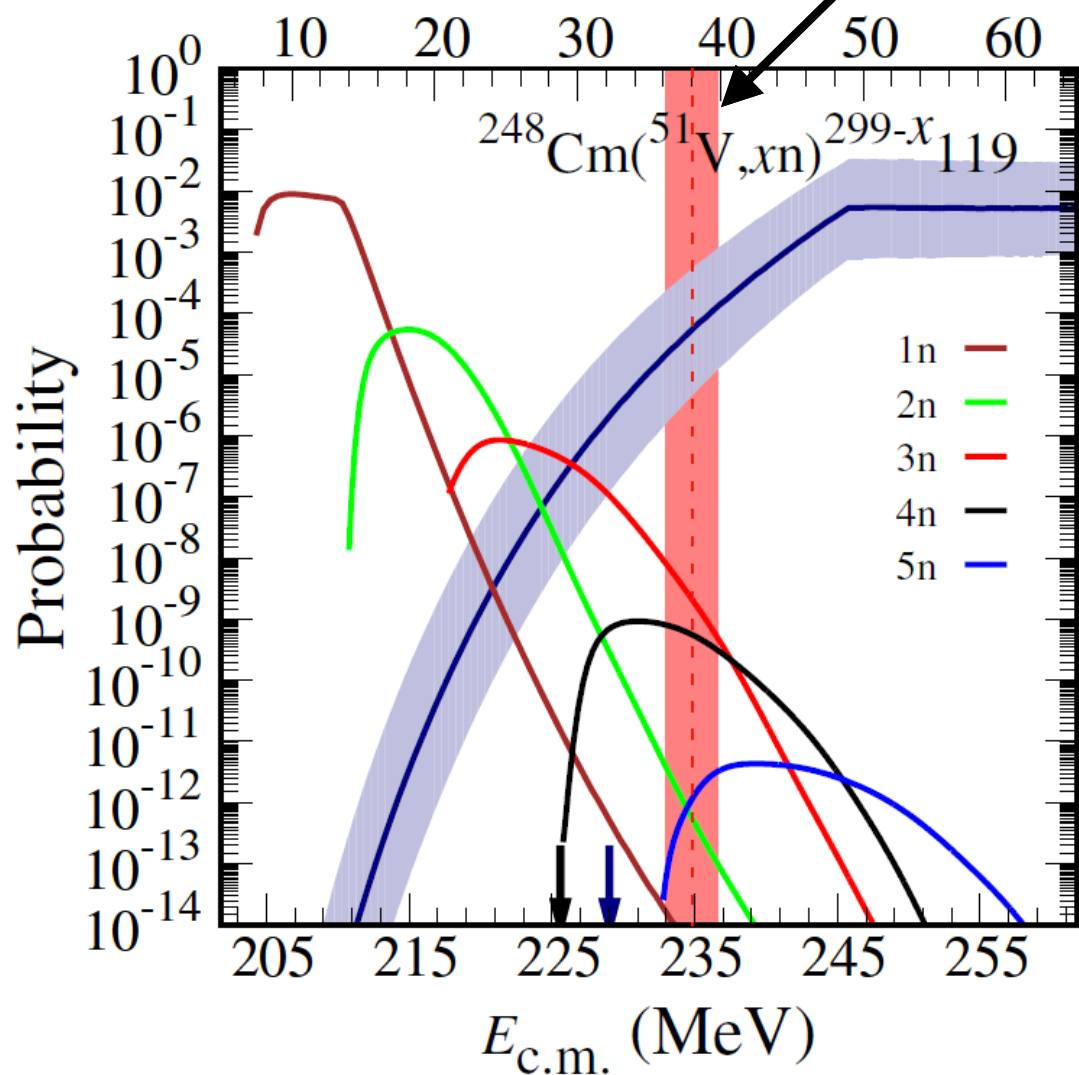
$B_0 = 229.03 \text{ MeV}$

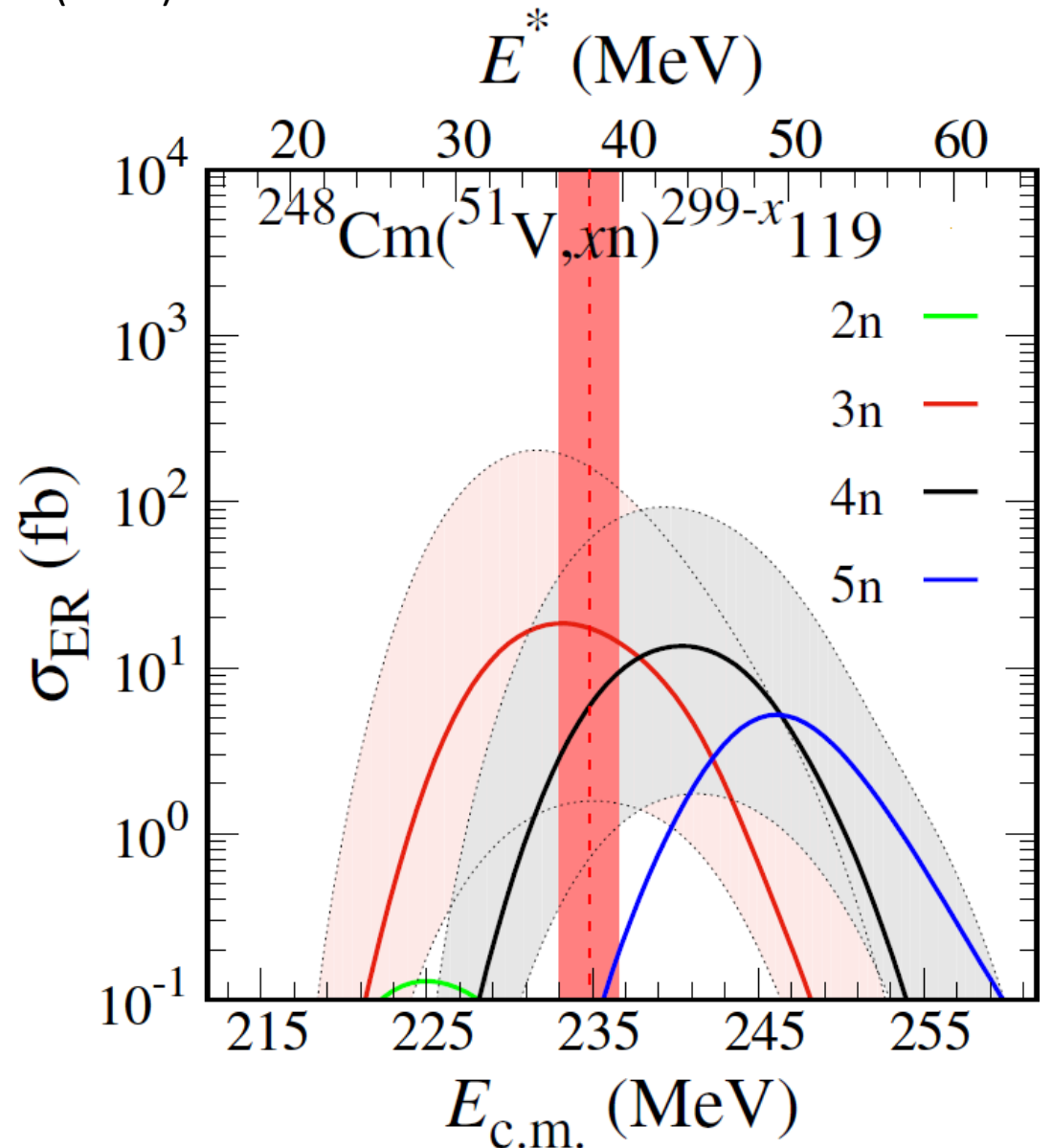
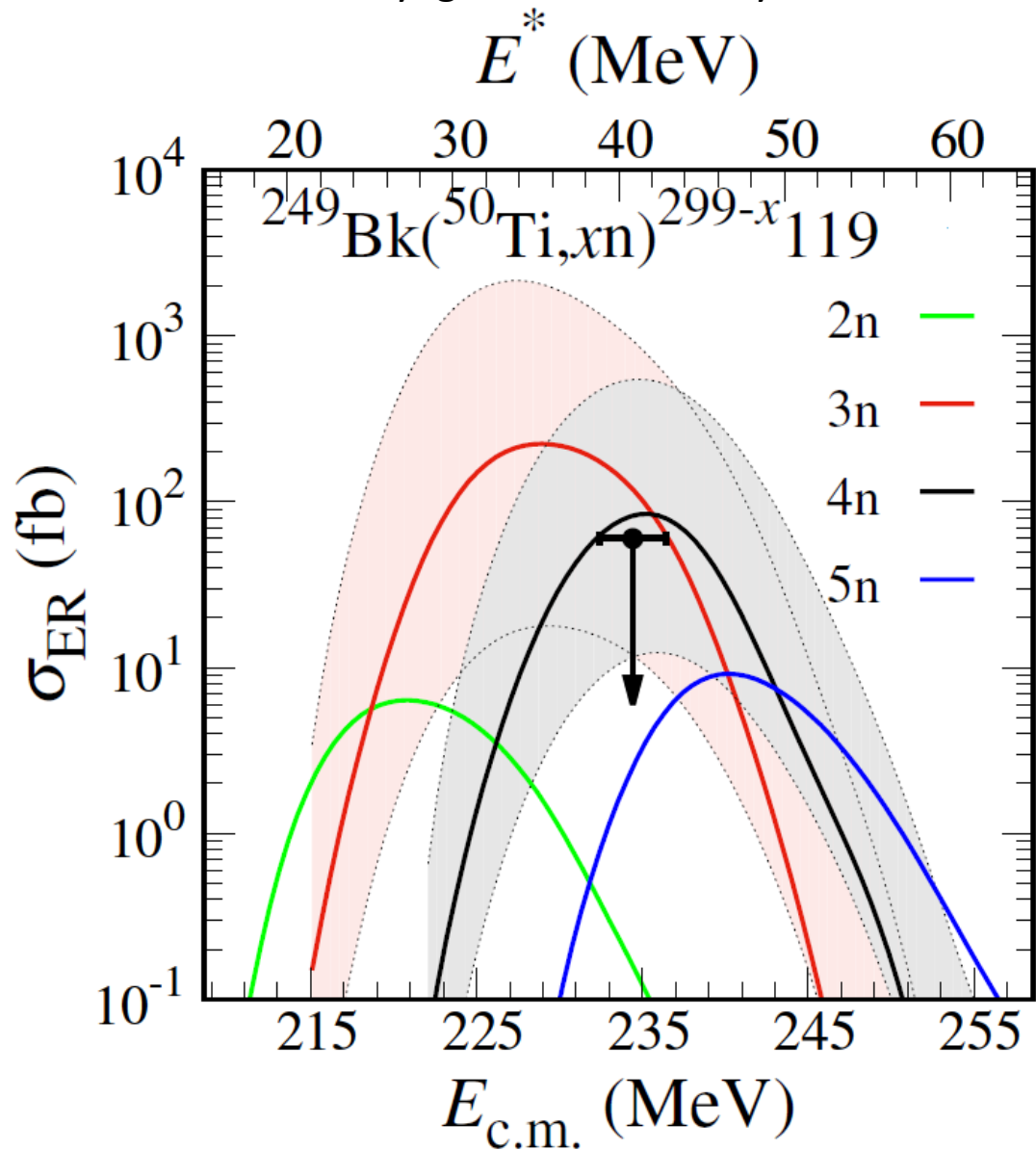
$\omega = 6.90 \text{ MeV}$

M. Tanaka *et al.*, J Phys. Soc. Jpn. 91, 084201 (2022)

E^* (MeV) $E_{c.m.} = 234.8 \pm 1.8 \text{ MeV}$

E^* (MeV)





Evaporation residue cross sections

Reactions $^{51}\text{V} + ^{248}\text{Cm}$ and $^{50}\text{Ti} + ^{249}\text{Bk}$ both lead to the same compound nucleus $^{299}119$, but with different cross sections.

$^{51}\text{V} + ^{248}\text{Cm}$

$^{50}\text{Ti} + ^{249}\text{Bk}$

^{48}Ca systematics

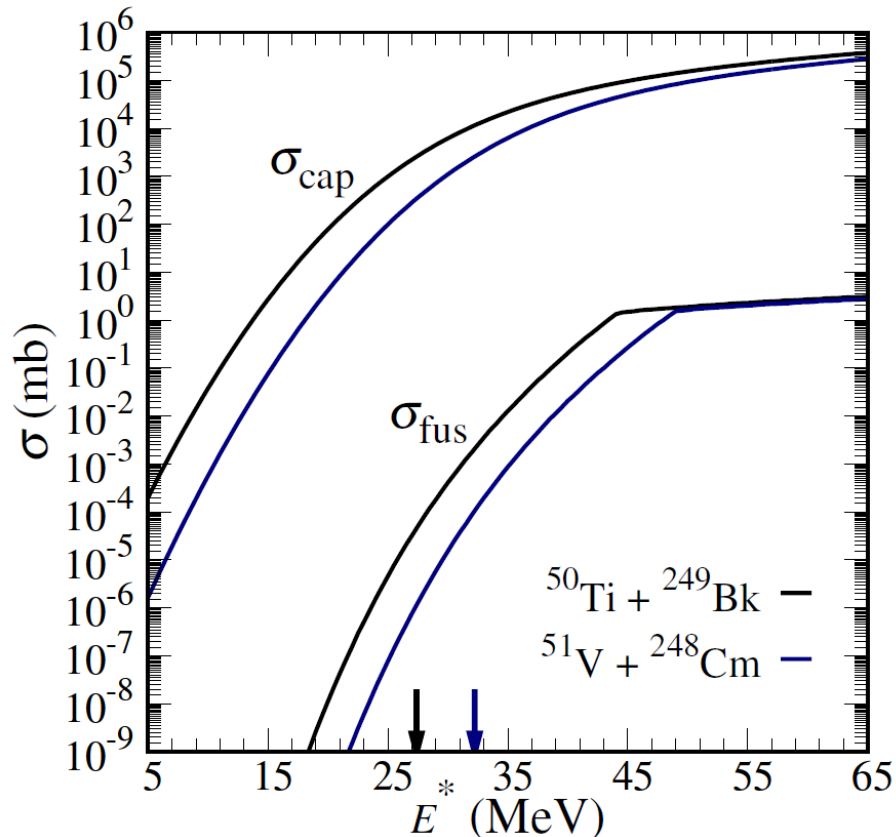
$$\sigma_{\text{MAX}}(3n) = 20 \text{ fb} \quad \sigma_{\text{MAX}}(4n) = 15 \text{ fb}$$

$$\sigma_{\text{MAX}}(3n) = 250 \text{ fb} \quad \sigma_{\text{MAX}}(4n) = 100 \text{ fb}$$

Lower limit – more probable values

$$\sigma(3n) = 2 \text{ fb} \quad \sigma(4n) = 2 \text{ fb}$$

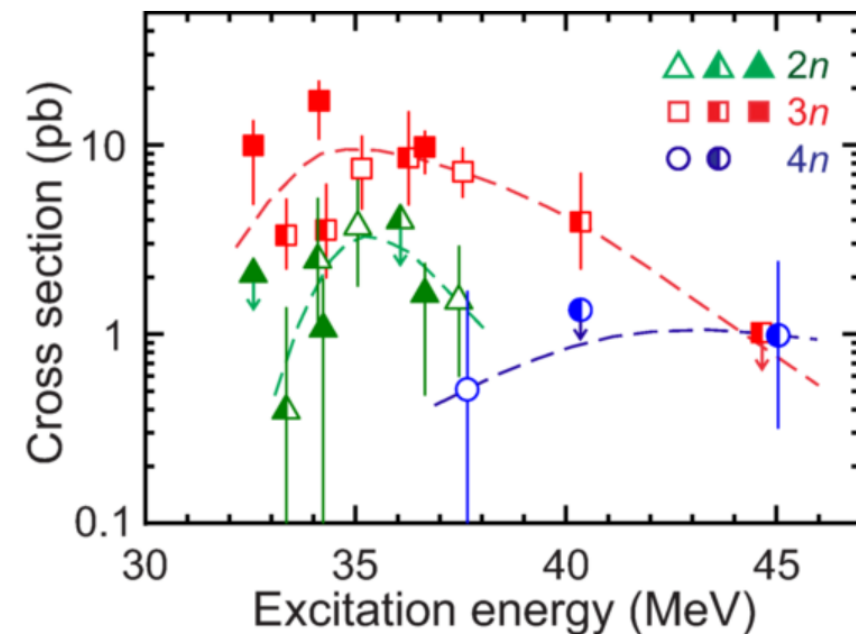
$$\sigma(3n) = 20 \text{ fb} \quad \sigma(4n) = 15 \text{ fb}$$



Entrance channel effect

$^{51}\text{V} + ^{248}\text{Cm}$ is more „charge symmetric“ than $^{50}\text{Ti} + ^{249}\text{Bk}$
 → greater Coulomb repulsion (8 MeV difference in B_0)

This makes the fusion cross section for the $^{51}\text{V} + ^{248}\text{Cm}$ reaction one order of magnitude smaller than for the $^{50}\text{Ti} + ^{249}\text{Bk}$ reaction at the excitation energies less than 45 MeV (3n and 4n channel).



First experiment at the Super Heavy Element Factory: High cross section of ^{288}Mc in the $^{243}\text{Am} + ^{48}\text{Ca}$ reaction and identification of the new isotope ^{264}Lr

Yu. Ts. Oganessian *et al.*

Phys. Rev. C **106**, L031301 – Published 29 September 2022

Search for element 120 in 2023?

$^{54}\text{Cr} + ^{248}\text{Cm}$

$\sigma(3n), \sigma(4n) < 1 \text{ fb}$

Low P_{surv}

NAJWIĘKSZYM ŻYJĄCYM WSPÓŁCZEŚNIE
TWÓRCĄ PIERWIASTKÓW JEST JURIJ OGA-
NIESIAN ZE ZJEDNOCZONEGO INSTYTUTU
BADAŃ JĄDROWYCH W DUBNEJ W ROSJI.

Współtworzyłem
ich dotąd 5!



Ha! Ja byłem Lepszy! Arr!

JURIJ JAKO JEDYNY ŻYJĄCY
CZŁOWIEK MA WŁASNY PIERWIASTEK.
UMIESZ GO ZNALEŹĆ?

Z PEWNOŚCIĄ BĘDĄ TWORZONE
KOLEJNE. MOŻE PEWNEGO DNIA TO
TY JAKIŚ ODKRYJESZ! TYLKO JAK GO
NAZWIESZ?

^{8}Og
GANESON

MOŻE
OD WŁASNEGO
NAZWISKA?

POWODZENIA!

Thank you for your attention



NATIONAL
CENTRE
FOR NUCLEAR
RESEARCH
ŚWIERK

www.ncbj.gov.pl

